Construction of $H(\mathrm{div})$-Conforming Mixed Finite Elements on Cuboidal Hexahedra

Todd Arbogast · **Zhen Tao**

Abstract We generalize the two dimensional mixed finite elements of Arbogast and Correa [T. Arbogast and M. R. Correa, SIAM J. Numer. Anal., 54 (2016), pp. 3332–3356] defined on quadrilaterals to three dimensional cuboidal hexahedra. The construction is similar in that polynomials are used directly on the element and supplemented with functions defined on a reference element and mapped to the hexahedron using the Piola transform. The main contribution is providing a systematic procedure for defining supplemental functions that are divergence-free and have any prescribed polynomial normal flux. General procedures are also presented for determining which supplemental normal fluxes are required to define the finite element space. Both full and reduced $H(\mathrm{div})$-approximation spaces may be defined, so the scalar variable, vector variable, and vector divergence are approximated optimally. The spaces can be constructed to be of minimal local dimension, if desired.

1 Introduction

It is well-known that standard mixed finite elements defined on a square or cube and mapped to a general convex quadrilateral or cuboidal hexahedron perform poorly;

Todd Arbogast
Department of Mathematics C1200, University of Texas, Austin, TX 78712-1202 and Institute for Computational Engineering and Sciences C0200, University of Texas, Austin, TX 78712-1229 E-mail: arbogast@ices.utexas.edu

Zhen Tao
Institute for Computational Engineering and Sciences C0200, University of Texas, Austin, TX 78712-1229
E-mail: taozhen.cn@gmail.com

in fact, they fail to approximate the divergence in an optimal way or require a very high number of local degrees of freedom. Recently, Arbogast and Correa [1] resolved the problem on quadrilaterals (although, see the 2004 paper [11] for the lowest order case). They defined two families of mixed finite elements that are of minimal local dimension and achieve optimal convergence properties. In this paper, we generalize these elements to convex, cuboidal hexahedra, i.e., convex polyhedra with six flat quadrilateral faces.

It is convenient to discuss $H(\text{div})$-conforming mixed finite elements in the context of the simplest problem to which they apply. Let $\Omega \subset \mathbb{R}^d$, $d = 2$ or 3, be a polytopal domain, let $W = L^2(\Omega)$ and $(\cdot, \cdot)_\omega$ denote the $L^2(\omega)$ or $(L^2(\omega))^d$ inner-product, and let $\mathbf{V} = H(\text{div}; \Omega) = \{\mathbf{v} \in (L^2(\Omega))^2 : \nabla \cdot \mathbf{u} \in L^2(\Omega)\}$. Consider the second order elliptic boundary value problem in mixed variational form: Find $(\mathbf{u}, p) \in \mathbf{V} \times W$ such that

$$(a^{-1}\mathbf{u}, \mathbf{v})_\Omega - (p, \nabla \cdot \mathbf{v})_\Omega = 0 \qquad \forall \mathbf{v} \in \mathbf{V}, \tag{1}$$

$$(\nabla \cdot \mathbf{u}, w)_\Omega = (f, w)_\Omega \quad \forall w \in W, \tag{2}$$

where $f \in L^2(\Omega)$ and the tensor a is uniformly positive definite and bounded. A mixed finite element method is given by restricting $\mathbf{V} \times W$ to inf-sup compatible finite element subspaces $\mathbf{V}_r \times W_r \subset \mathbf{V} \times W$ defined (in our case) over a mesh of convex, cuboidal hexahedra, where $r \geq 0$ is the index of the subspaces.

Full $H(\text{div})$-approximation spaces of index $r \geq 0$ approximate $\mathbf{u}$, p, and $\nabla \cdot \mathbf{u}$ to order h^{r+1}, where h is the maximal diameter of the computational mesh elements. Such spaces include the classic spaces of Raviart-Thomas (RT) [16, 19] in 2-D and 3-D, as well as, in 2-D only, the spaces of Arnold-Boffi-Falk (ABF) [4] and Arbogast-Correa (AC) [1]. The ABF spaces have been generalized recently to 3-D by Bergot and Durufle [6]. Reduced $H(\text{div})$-approximation spaces of index $r \geq 1$ approximate $\mathbf{u}$ to order h^{r+1} and p and $\nabla \cdot \mathbf{u}$ to order h^r. In this category are the classic spaces due to Brezzi-Douglas-Marini (BDM) [8] in 2-D and their 3-D counterpart from Brezzi-Douglas-Duràn-Fortin (BDDF) [7, 2], as well as the reduced Arbogast-Correa (AC$^{\text{red}}$) spaces [1] in 2-D. Recent progress on defining 3-D mixed finite elements has been made by many authors, including, but certainly not exhaustively, [12, 6, 2, 3, 10].

All spaces save AC, AC$^{\text{red}}$, and the spaces of Cockburn and Fu [10] are defined on a reference square or cube $\hat{E} = [0, 1]^d$ and mapped to the element E using the Piola transform. The RT and BDM (and BDDF) spaces lose accuracy. The ABF spaces maintain accuracy, but at the expense of adding many extra degrees of freedom to the local finite element space. Cockburn and Fu construct finite elements on hexahedra using a sub mesh of tetrahedra.

The two families of AC spaces, $\mathbf{V}_r$ and $\mathbf{V}_r^{\text{red}}$, are constructed using a different strategy. They use polynomials defined directly on the element and supplemented by two (one if $r = 0$) basis functions defined on a reference square and mapped via Piola. Let $\mathbb{P}_r$ denote the space of polynomials of degree up to r, and let $\tilde{\mathbb{P}}_r$ denote the space of homogeneous polynomials of exact degree r. On a convex quadrilateral element E, for which $d = 2$ and $\mathbf{x} = (x_1, x_2)$, the full $H(\text{div})$-approximation spaces of index $r \geq 0$ are

$$\mathbf{V}_r(E) = (\mathbb{P}_r)^d \oplus \mathbf{x}\tilde{\mathbb{P}}_r \oplus \mathbb{S}_r(E) \quad \text{and} \quad W_r(E) = \mathbb{P}_r, \tag{3}$$

and the reduced $H(\text{div})$-approximation spaces of index $r \geq 1$ are

$$\mathbf{V}_r^{\text{red}}(E) = (\mathbb{P}_r)^d \oplus \mathbb{S}_r(E) \quad \text{and} \quad W_r(E) = \mathbb{P}_{r-1}. \tag{4}$$

One can define the reference supplemental space on $\hat{E} = [0,1]^2$ in 2-D as

$$\hat{\mathbb{S}}_r = \begin{cases} \text{span}\{\widehat{\text{curl}}((\hat{x}_1 - 1/2)(\hat{x}_2 - 1/2))\}, & r = 0, \\ \text{span}\{\widehat{\text{curl}}((\hat{x}_1 - 1/2)^{r-1}\hat{x}_1(1 - \hat{x}_1)(\hat{x}_2 - 1/2)), & \\ \quad \widehat{\text{curl}}((\hat{x}_1 - 1/2)(\hat{x}_2 - 1/2)^{r-1}\hat{x}_2(1 - \hat{x}_2))\}, & r \geq 1, \end{cases} \tag{5}$$

and then

$$\mathbb{S}_r(E) = \mathscr{P}_E \hat{\mathbb{S}}_r, \tag{6}$$

where $\mathscr{P}_E$ is the Piola transform from $\hat{E} = [0,1]^d$ to E.

Our generalization of the two families of AC spaces to the case of a convex, cuboidal hexahedron E gives full and reduced $H(\text{div})$-approximating mixed finite elements $\mathbf{V}(E) \times W(E)$ and $\mathbf{V}^{\text{red}}(E) \times W(E)$, respectively. These are defined to include spaces of polynomials and special supplemental functions. In fact, the spaces are defined formally by the same equations (3)–(4), (6), except that now $d = 3$, $\mathbf{x} = (x_1, x_2, x_3)$, and the supplemental space $\mathbb{S}_r(E)$ or $\hat{\mathbb{S}}_r$ (replacing (5)) must be defined carefully. The number of supplemental functions is 2 for $r = 0$ and otherwise at most $3(r+1)$. The divergences of these vectors lie in $\mathbb{P}_r$ for the full space and in $\mathbb{P}_{r-1}$ for the reduced space, and the normal flux on each edge or face f of E is in $\mathbb{P}_r(f)$ (i.e., $\mathbb{P}_r$ in dimension $d-1$). In fact, the degrees of freedom (DOFs) of a vector $\mathbf{v} \in \mathbf{V}_r$ or $\mathbf{V}_r^{\text{red}}$ include the divergence and edge or face normal fluxes:

$$(\nabla \cdot \mathbf{v}, w)_E \quad \forall w \in \mathbb{P}_r^* \text{ (for } \mathbf{V}_r) \text{ or } \mathbb{P}_{r-1}^* \text{ (for } \mathbf{V}_r^{\text{red}}), \tag{7}$$

$$(\mathbf{v} \cdot \nu, \mu)_f \quad \forall \text{ edges } (d = 2) \text{ or faces } (d = 3) f \text{ of } E \text{ and } \forall \mu \in \mathbb{P}_r(f), \tag{8}$$

where ν is the outer unit normal vector to E and $\mathbb{P}_r^*$ are the polynomials of degree r with no constant term. The purpose of the supplements is to make these DOFs independent, so that the elements can be joined in $H(\text{div})$ to form $\mathbf{V}_r$ or $\mathbf{V}_r^{\text{red}}$ while also maintaining consistency to approximate the divergence. The set of DOFs is completed by adding conditions on the interior, divergence-free, bubble functions (for $H(\text{div})$-conforming elements, an *interior bubble function* is a vector function with vanishing normal component on ∂E).

After setting some additional notation in Section 2, we describe how to construct arbitrary, divergence-free supplemental functions in 3-D with a prescribed normal flux in Sections 3 and 4. In Section 5, we describe a way to choose the specific supplemental function space $\hat{\mathbb{S}}_r$ needed to define $\mathbb{S}_r(E)$ by (6). The most useful cases $r = 0$ and $r = 1$ are given in detail (although some proofs are relegated to the appendices). For $r \geq 1$, we need to determine the normal fluxes needed to ensure that the DOFs (8) are independent. We note the recent work of Cockburn and Fu [10] in this regard, but we provide a method for resolving this issue based on linear algebra. We present some numerical results in Section 6. We close by summarizing our results in the last section.

2 Further notation

In this section, we fix the notation and geometry used throughout the paper. As noted above, let $\mathbb{P}_r$ denote the space of polynomials of degree r. Generally, $\mathbb{P}_r = \mathbb{P}_r(\mathbb{R}^3)$ is defined over a three-dimensional domain. Sometimes we need to restrict polynomials to faces, so let $\mathbb{P}_r(f)$ be the polynomials defined over the domain f. Let $\tilde{\mathbb{P}}_r$ denote the space of homogeneous polynomials of degree r. We also let $\mathbb{P}_{r,s,t}$ denote the tensor product polynomial spaces of degree r in x_1, s in x_2, and t in x_3.

2.1 A convex, cuboidal hexahedron and the Piola map

Fix the reference element $\hat{E} = [0,1]^3$ and take any convex, cuboidal hexahedron E oriented as in Figure 1. The reference element $\hat{E}$ has faces ordered as follows. Face 0 is where $\hat{x}_1 = 0$ and it is denoted $\hat{f}_0 = E \cap \{\hat{x}_1 = 0\}$, face 1 is where $\hat{x}_1 = 1$ and it is denoted $\hat{f}_1$, and so forth to face 5 is where $\hat{x}_3 = 1$ and it is denoted $\hat{f}_5$. The vertices $\hat{\mathbf{x}}_{ijk}$ are indexed by the faces of intersection, i.e., $\hat{\mathbf{x}}_{ijk} = \hat{f}_i \cap \hat{f}_j \cap \hat{f}_k$. The bijective and trilinear map $\mathbf{F}_E : \hat{E} \to E$ is defined by

$$
\begin{aligned}
\mathbf{F}_E(\hat{\mathbf{x}}) = {}& \mathbf{x}_{024}(1-\hat{x}_1)(1-\hat{x}_2)(1-\hat{x}_3) + \mathbf{x}_{124}\hat{x}_1(1-\hat{x}_2)(1-\hat{x}_3) \\
& + \mathbf{x}_{034}(1-\hat{x}_1)\hat{x}_2(1-\hat{x}_3) + \mathbf{x}_{134}\hat{x}_1\hat{x}_2(1-\hat{x}_3) \\
& + \mathbf{x}_{025}(1-\hat{x}_1)(1-\hat{x}_2)\hat{x}_3 + \mathbf{x}_{125}\hat{x}_1(1-\hat{x}_2)\hat{x}_3 \\
& + \mathbf{x}_{035}(1-\hat{x}_1)\hat{x}_2\hat{x}_3 + \mathbf{x}_{135}\hat{x}_1\hat{x}_2\hat{x}_3 \\
& \in \mathbb{P}_{1,1,1}.
\end{aligned}
\tag{9}
$$

This map fixes the notation on E (faces $f_i = \mathbf{F}_E(\hat{f}_i)$ and vertices $\mathbf{x}_{ijk} = \mathbf{F}_E(\hat{\mathbf{x}}_{ijk})$). The center of face i is denoted $\mathbf{x}_i$. The outer unit normal to face i is $\nu_i = (\nu_{i,1}, \nu_{i,2}, \nu_{i,3})$. For example,

$$
\nu_1 = \frac{(\mathbf{x}_{134} - \mathbf{x}_{124}) \times (\mathbf{x}_{125} - \mathbf{x}_{124})}{\|(\mathbf{x}_{134} - \mathbf{x}_{124}) \times (\mathbf{x}_{125} - \mathbf{x}_{124})\|}.
\tag{10}
$$

2.1.1 Piola transform and Jacobians

Let $D\mathbf{F}_E(\hat{\mathbf{x}})$ denote the Jacobian matrix of F_E and $J_E(\hat{\mathbf{x}}) = \det(D\mathbf{F}_E(\hat{\mathbf{x}}))$. The contravariant Piola transform $\mathscr{P}_E$ maps a vector $\hat{\mathbf{v}} : \hat{E} \to \mathbb{R}^2$ to a vector $\mathbf{v} : E \to \mathbb{R}^2$ by the formula

$$
\mathbf{v}(\mathbf{x}) = \mathscr{P}_E(\hat{\mathbf{v}})(\mathbf{x}) = \frac{1}{J_E}D\mathbf{F}_E\hat{\mathbf{v}}(\hat{\mathbf{x}}), \quad \text{where } \mathbf{x} = \mathbf{F}_E(\hat{\mathbf{x}}).
\tag{11}
$$

For a scalar function w, we define the map $\hat{w}$ by $\hat{w}(\hat{\mathbf{x}}) = w(\mathbf{x})$, where again $\mathbf{x} = \mathbf{F}_E(\hat{\mathbf{x}})$.

The Piola transform preserves the divergence and normal components of $\hat{\mathbf{v}}$ in the sense that

$$
\nabla \cdot \mathbf{v} = \frac{1}{J_E}\hat{\nabla} \cdot \hat{\mathbf{v}},
\tag{12}
$$

$$
\mathbf{v} \cdot \nu = \frac{1}{K_i}\hat{\mathbf{v}} \cdot \hat{\nu} \quad \text{for each face } f_i \text{ of } \partial E,
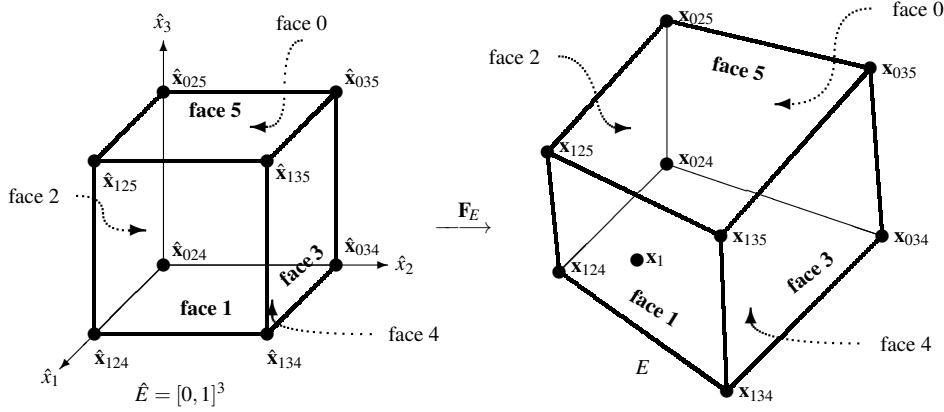\tag{13}
$$

Fig. 1 The geometry of the cuboidal hexahedron. On the left is the reference $\hat{E} = [0,1]^3$, which is trilinearly mapped to the hexahedron E. The faces are labeled from 0 to 5, and faces 1, 3, and 5 are in front. The corner points are labeled by their intersections with the faces (e.g., $\mathbf{x}_{135}$ intersects faces 1, 3, and 5). The centers of the faces are labeled by the face (we show only $\mathbf{x}_1$ on face 1).

where K_i is the face Jacobian. The face Jacobian for face i is

$$
K_i = \left\| \left(\frac{\partial \mathbf{F}_E}{\partial \hat{x}_\ell} \times \frac{\partial \mathbf{F}_E}{\partial \hat{x}_m} \right) \Big|_{f_i} \right\| = \left| \left(\frac{\partial \mathbf{F}_E}{\partial \hat{x}_\ell} \times \frac{\partial \mathbf{F}_E}{\partial \hat{x}_m} \right) \Big|_{f_i} \cdot v_i \right|,
\tag{14}
$$

where i, ℓ, and m are distinct integers from $\{1,2,3\}$ and, say, $\ell < m$. The face Jacobian describes the bilinear distortion of the face, and it depends only on the face vertices (so two elements intersecting at face f will have the same face Jacobian). If we re-index the face so that

$$
\mathbf{F}_E(\hat{x}_\ell, \hat{x}_m)\big|_{f_i} = \mathbf{y}_0(1 - \hat{x}_\ell)(1 - \hat{x}_m) + \mathbf{y}_1 \hat{x}_\ell(1 - \hat{x}_m)
$$
$$
+ \mathbf{y}_2(1 - \hat{x}_\ell)\hat{x}_m + \mathbf{y}_3 \hat{x}_\ell \hat{x}_m,
\tag{15}
$$

then it is not hard to show, when f_i is flat, that

$$
\begin{aligned}
K_i(\hat{x}_\ell, \hat{x}_m) = \quad & \|(\mathbf{y}_2 - \mathbf{y}_0) \times (\mathbf{y}_1 - \mathbf{y}_0)\|(1 - \hat{x}_\ell)(1 - \hat{x}_m) \\
& + \|(\mathbf{y}_3 - \mathbf{y}_1) \times (\mathbf{y}_0 - \mathbf{y}_1)\|\hat{x}_\ell(1 - \hat{x}_m) \\
& + \|(\mathbf{y}_3 - \mathbf{y}_2) \times (\mathbf{y}_0 - \mathbf{y}_2)\|(1 - \hat{x}_\ell)\hat{x}_m \\
& + \|(\mathbf{y}_2 - \mathbf{y}_3) \times (\mathbf{y}_1 - \mathbf{y}_3)\|\hat{x}_\ell \hat{x}_m \\
& \in \mathbb{P}_{1,1}.
\end{aligned}
\tag{16}
$$

2.1.2 Local variables

It is clear that for the reference cube $\hat{E}$, the local variables can be taken as $\hat{x}_2$ and $\hat{x}_3$ on faces 0 and 1, $\hat{x}_1$ and $\hat{x}_3$ on faces 2 and 3, and $\hat{x}_1$ and $\hat{x}_2$ on faces 4 and 5. Similar indexing does not necessarily hold on E. In fact, faces indexed as being opposite to each other may be far from parallel (they could even be perpendicular to each other).

It is necessary to select local variables on each face of E, two from among the set of variables $\{x_1, x_2, x_3\}$. For face ℓ, we denote these variables by (x_{i_ℓ}, x_{j_ℓ}), where we tacitly assume that $i_\ell < j_\ell$. In practice, one can find the maximal absolute component of v_ℓ, say $|v_{\ell,m}|$, and omit x_m from the set $\{x_1, x_2, x_3\}$, leaving the local coordinates $\{x_{i_\ell}, x_{j_\ell}\}$.

3 Construction of Pre-supplemental Functions on the Reference Cube

In this section, we construct a vector function on the reference cube $\hat{E} = [0,1]^3$ with a vanishing divergence and prescribed monomial normal flux (up to a constant). These functions will be used later to construct the space of supplements $\mathbb{S}_r(E)$ for the new mixed finite elements. We call our special vector functions *pre-supplements*. For simplicity, we consider only face 1 (where $\hat{x}_1 = 1$). The other faces are handled analogously.

The vector functions in the local BDDF spaces of index r [7,2] have the property that their normal fluxes are polynomials of degree r. Moreover, both the normal fluxes and the divergence are degrees of freedom. Analogous to BDDF, we can define vector functions with the properties we desire. Let us fix the monomial as $\hat{x}_2^\ell \hat{x}_3^m$ for some integers $\ell \geq 0$ and $m \geq 0$. We define the pre-supplement to be, when $\ell + m \geq 1$,

$$\hat{\psi}_{\ell,m}^1 = \begin{pmatrix} \hat{x}_1 \hat{x}_2^\ell \hat{x}_3^m - \dfrac{\hat{x}_1}{(\ell+1)(m+1)} \\ \dfrac{1}{2(\ell+1)} \hat{x}_2 (1 - \hat{x}_2^\ell) \left(\hat{x}_3^m + \dfrac{1}{m+1} \right) \\ \dfrac{1}{2(m+1)} \hat{x}_3 (1 - \hat{x}_3^m) \left(\hat{x}_2^\ell + \dfrac{1}{\ell+1} \right) \end{pmatrix} \in \mathbb{P}_{\ell+m+1}^3(\hat{E}). \tag{17}$$

It can be readily verified that indeed this function lies in the more symmetric BDDF space as defined by Arnold and Awanou [2], although this fact is not important in itself. What is important is that we have our desired properties

$$\hat{\nabla} \cdot \hat{\psi}_{\ell,m}^1 = 0 \quad \text{and} \quad \hat{\psi}_{\ell,m}^1 \cdot \hat{v} = \begin{cases} \hat{x}_2^\ell \hat{x}_3^m - \dfrac{1}{(\ell+1)(m+1)} & \text{on } \hat{f}_1, \ \ell + m \geq 1, \\ 0 & \text{on } \hat{f}_i, \ i = 0, 2, \ldots, 5, \end{cases} \tag{18}$$

where we recall that the face f_1 is where $\hat{x}_1 = 1$. The case $\ell = m = 0$ reduces to the zero vector because of the divergence theorem. We therefore accept a constant divergence and simply take

$$\hat{\psi}_{0,0}^1 = \begin{pmatrix} \hat{x}_1 \\ 0 \\ 0 \end{pmatrix}, \tag{19}$$

for which

$$\hat{\nabla} \cdot \hat{\psi}_{0,0}^1 = 1 \quad \text{and} \quad \hat{\psi}_{0,0}^1 \cdot \hat{v} = \begin{cases} 1 & \text{on } \hat{f}_1, \\ 0 & \text{on } \hat{f}_i, \ i = 0, 2, \ldots, 5. \end{cases} \tag{20}$$

We can construct similar pre-supplements for each face; label these as $\hat{\psi}^i_{\ell,m}$ for face $i = 0, 1, \ldots, 5$.

We remark that our pre-supplemental functions are not unique when there are divergence-free bubble functions. For example, to $\hat{\psi}^1_{\ell,m}$, one could add any function of the form

$$
\begin{pmatrix}
0 \\
\dfrac{\partial}{\partial \hat{x}_3} \left[\hat{x}_2 (1 - \hat{x}_2) \hat{x}_3 (1 - \hat{x}_3) \hat{p} \right] \\
-\dfrac{\partial}{\partial \hat{x}_2} \left[\hat{x}_2 (1 - \hat{x}_2) \hat{x}_3 (1 - \hat{x}_3) \hat{p} \right]
\end{pmatrix},
\tag{21}
$$

where $\hat{p}$ is any polynomial in $\hat{x}_2$ and $\hat{x}_3$, and we would maintain (18).

4 Construction of the Supplemental Functions on Hexahedra

In this section, we construct a supplemental vector function σ with zero divergence on the convex, cuboidal hexahedron E. It has a prescribed polynomial normal flux (up to a constant) on a single face and vanishing normal flux on the other 5 faces. We continue to fix the nonzero flux on face 1 for ease of exposition; the other faces are handled similarly. In terms of the local face variables (x_{i_1}, x_{j_1}), suppose that the prescribed flux is $x^\ell_{i_1} x^m_{j_1}$. That is, we want to define $\sigma^1_{\ell,m}$ when $\ell + m \geq 1$ so that, for some constant $c^1_{\ell,m}$,

$$
\nabla \cdot \sigma^1_{\ell,m} = 0 \quad \text{and} \quad \sigma^1_{\ell,m} \cdot \nu =
\begin{cases}
x^\ell_{i_1} x^m_{j_1} - c^1_{\ell,m} & \text{on } f_1, \ \ell + m \geq 1, \\
0 & \text{on } f_i, \ i = 0, 2, \ldots, 5.
\end{cases}
\tag{22}
$$

The construction is given by first defining an appropriate vector function $\hat{\sigma}^1_{\ell,m}$ on the reference cube $\hat{E}$ and then mapping it to E using the Piola transform (11), so that $\sigma^1_{\ell,m} = \mathscr{P}_E \hat{\sigma}^1_{\ell,m}$. The key is to recognize that the normal components of $\hat{\sigma}^1_{\ell,m}$ transform by (13), and therefore we need to include the factor K_1 within the first row of $\hat{\sigma}^1_{\ell,m}$. Our construction is vaguely reminiscent of the one given in 2-D by Shen [17] (for which the resulting method was later proved in [14]).

To proceed, we must realize two simple facts. First, the face Jacobian K_1 is bilinear in the reference variables, i.e., (16) holds. Second, the polynomial flux $x^\ell_{i_1} x^m_{j_1}$ is evaluated in terms of the reference variables by the map $F_E : \hat{E} \to E$ (9), i.e.,

$$
x_{i_1} = F_{i_1}(1, \hat{x}_2, \hat{x}_3) \quad \text{and} \quad x_{j_1} = F_{j_1}(1, \hat{x}_2, \hat{x}_3),
\tag{23}
$$

which are both bilinear. Therefore the product $x^\ell_{i_1} x^m_{j_1}$, multiplied by K_1 and written in terms of the reference variables, is in the space $\mathbb{P}_{n+1,n+1}$, where $n = \ell + m$. Let the pre-image of $x^\ell_{i_1} x^m_{j_1}$ (scaled by K_1) be denoted

$$
\begin{aligned}
K_1 x^\ell_{i_1} x^m_{j_1} &= K_1(\hat{x}_2, \hat{x}_3) F_{i_1}(1, \hat{x}_2, \hat{x}_3)^\ell F_{j_1}(1, \hat{x}_2, \hat{x}_3)^m \\
&= \sum_{\substack{i=0 \\ i+j \geq 1}}^{n+1} \sum_{j=0}^{n+1} \alpha^{\ell,m}_{ij} \left(\hat{x}^i_2 \hat{x}^j_3 - \frac{1}{(i+1)(j+1)} \right) + \alpha^{\ell,m}_{0,0}.
\end{aligned}
\tag{24}
$$

That is, in practice, we compute the coefficients $\alpha_{ij}^{\ell,m}$ based on the geometry of the hexahedron.

When $n = \ell = m = 0$, let

$$\hat{\sigma}_{0,0}^1 = \sum_{i=0}^{1} \sum_{j=0}^{1} \alpha_{ij}^{0,0} \hat{\psi}_{i,j}^1. \tag{25}$$

Recalling (18) and (20), this function has divergence $\alpha_{0,0}^{0,0}$ and flux K_1 on face 1. By the divergence theorem, clearly $\alpha_{0,0}^{0,0} = |f_1|$, the area of face 1, so

$$\hat{\nabla} \cdot \hat{\sigma}_{0,0}^1 = |f_1| \quad \text{and} \quad \hat{\sigma}_{0,0}^1 \cdot \hat{v} = \begin{cases} K_1 & \text{on } \hat{f}_1, \\ 0 & \text{on } \hat{f}_i, \ i = 0, 2, \ldots, 5. \end{cases} \tag{26}$$

When $n = \ell + m \geq 1$, we define

$$\hat{\sigma}_{\ell,m}^1 = \sum_{i=0}^{n+1} \sum_{j=0}^{n+1} \alpha_{ij}^{\ell,m} \hat{\psi}_{i,j}^1 - \frac{\alpha_{0,0}^{\ell,m}}{|f_1|} \hat{\sigma}_{0,0}^1, \tag{27}$$

which has vanishing divergence and matches the flux (24), up to a constant multiple of K_1. Owing to (12)–(13), $\sigma_{\ell,m}^1 = \mathscr{P}_E \hat{\sigma}_{\ell,m}^1$ has the desired properties (22). We can construct a similar vector function for each face; label these as $\sigma_{\ell,m}^i$ for face $i = 0, 1, \ldots, 5$.

In the case of constant normal face fluxes (i.e., $n = 0$), we cannot remove the divergence unless we allow nonzero flux on at least two faces. We therefore define and later use the lowest order divergence-free supplements given by

$$\sigma_{0,0}^{i,j} = \mathscr{P}_E \left(\frac{\hat{\sigma}_{0,0}^i}{|f_i|} - \frac{\hat{\sigma}_{0,0}^j}{|f_j|} \right). \tag{28}$$

Using (12), (13) and (26), it can be easily verified that $\sigma_{0,0}^{i,j}$ is divergence-free and provides constant normal fluxes on faces i and j.

5 Generalized AC Spaces on Convex, Cuboidal Hexahedra

We now present our generalization of the two families of AC spaces [1]. The full and reduced spaces are given by (3) and (4), respectively, once we have defined the supplemental space $\mathbb{S}_r$ for $r \geq 0$, so that the DOFs (7)–(8) are independent.

The supplemental space is constructed using the functions defined in Sections 3–4, once we know what fluxes are required to independently span the space of normal fluxes (8). To this end, it is convenient to define the full flux operator $\mathscr{F}$ as well as

the operators $\mathscr{F}_{024}$ and $\mathscr{F}_{135}$ on the even and odd faces, respectively, to be

$$\mathscr{F}(\mathbf{u}) = \left[\mathbf{u} \cdot v_0|_{f_0}, \; \dots \; \mathbf{u} \cdot v_5|_{f_5}\right] \quad \subset \prod_{i=0}^{5} \mathbb{P}_r(f_i) = (\mathbb{P}_r(\mathbb{R}^2))^{1\times 6}, \qquad (29)$$

$$\mathscr{F}_{024}(\mathbf{u}) = \left[\mathbf{u} \cdot v_0|_{f_0}, \mathbf{u} \cdot v_2|_{f_2}, \mathbf{u} \cdot v_4|_{f_4}\right] \subset \prod_{i=0}^{2} \mathbb{P}_r(f_{2i}) = (\mathbb{P}_r(\mathbb{R}^2))^{1\times 3},$$

$$\mathscr{F}_{135}(\mathbf{u}) = \left[\mathbf{u} \cdot v_1|_{f_1}, \mathbf{u} \cdot v_3|_{f_3}, \mathbf{u} \cdot v_5|_{f_5}\right] \subset \prod_{i=0}^{2} \mathbb{P}_r(f_{2i+1}) = (\mathbb{P}_r(\mathbb{R}^2))^{1\times 3},$$

Note that $\mathscr{F}$ is a permutation of the block matrix $\begin{bmatrix} \mathscr{F}_{024} & \mathscr{F}_{135} \end{bmatrix}$. For a sequence of n functions, we also define the "flux matrix" as

$$\mathscr{F}(\mathbf{u}_1, \dots, \mathbf{u}_n) = \begin{bmatrix} \mathscr{F}(\mathbf{u}_1) \\ \vdots \\ \mathscr{F}(\mathbf{u}_n) \end{bmatrix} = \begin{bmatrix} \mathbf{u}_1 \cdot v_0|_{f_0} & \dots & \mathbf{u}_1 \cdot v_5|_{f_5} \\ \vdots & \ddots & \vdots \\ \mathbf{u}_n \cdot v_0|_{f_0} & \dots & \mathbf{u}_n \cdot v_5|_{f_5} \end{bmatrix} \in (\mathbb{P}_r(\mathbb{R}^2))^{n\times 6}, \qquad (30)$$

and we define $\mathscr{F}_{024}(\mathbf{u}_1, \dots, \mathbf{u}_n)$ and $\mathscr{F}_{135}(\mathbf{u}_1, \dots, \mathbf{u}_n)$ in $(\mathbb{P}_r(\mathbb{R}^2))^{n\times 3}$ analogously.

5.1 The case $r = 0$

On the convex, cuboidal hexahedron E, the new space is

$$\mathbf{V}_0(E) = \mathbb{P}_0^3 \oplus \mathbf{x}\mathbb{P}_0 \oplus \mathbb{S}_0, \qquad (31)$$

which has only normal flux DOFs. We will give two definitions of $\mathbb{S}_0$, but first, note that $\mathbb{P}_0^3 \oplus \mathbf{x}\mathbb{P}_0$ has local dimension four, and a basis is

$$\mathscr{B}_0^{\mathrm{poly}} = \{\mathbf{x} - \mathbf{x}_{124}, \mathbf{x} - \mathbf{x}_{034}, \mathbf{x} - \mathbf{x}_{025}, \mathbf{x} - \mathbf{x}_{024}\}. \qquad (32)$$

The normal flux $(\mathbf{x} - \mathbf{x}_{ijk}) \cdot v_\ell|_{f_\ell}$ is zero if $\ell \in \{i, j, k\}$ and strictly positive otherwise.

5.1.1 A simple supplemental space for $r = 0$

Recalling (28), we define simply

$$\mathbb{S}_0^{\mathrm{simple}} = \mathrm{span}\{\sigma_{0,0}^{1,3}, \sigma_{0,0}^{3,5}\}. \qquad (33)$$

A local basis is $\mathscr{B}_0^{\mathrm{simple}} = \mathscr{B}_0^{\mathrm{poly}} \cup \{\sigma_{0,0}^{1,3}, \sigma_{0,0}^{3,5}\}$. To prove that the DOFs are independent, we compute the flux matrix, which is an ordinary matrix of numbers when $r = 0$. This matrix is a permutation of $\begin{bmatrix} \mathscr{F}_{024} & \mathscr{F}_{135} \end{bmatrix}$, which has the sign

$$\mathrm{signum}\left(\begin{bmatrix} \mathscr{F}_{024}(\mathscr{B}_0^{\mathrm{simple}}) & \mathscr{F}_{135}(\mathscr{B}_0^{\mathrm{simple}}) \end{bmatrix}\right) = \left[\begin{array}{ccc|ccc} + & 0 & 0 & 0 & + & + \\ 0 & + & 0 & + & 0 & + \\ 0 & 0 & + & + & + & 0 \\ \hline 0 & 0 & 0 & + & + & + \\ 0 & 0 & 0 & + & - & 0 \\ 0 & 0 & 0 & 0 & + & - \end{array}\right], \qquad (34)$$

where a plus or minus sign ($+$ or $-$) indicates that the number is strictly positive or negative, respectively. Obviously, matrix (34) is invertible if the determinant of the lower right 3×3 submatrix is nonzero. This determinant is strictly positive if we expand the 3×3 matrix by Sarrus' rule. Since a matrix of this form is invertible, we can decouple the DOFs (8); thus, the mixed finite element is well defined.

A set of shape functions can be defined by inverting $\mathscr{F}(\mathscr{B}_0^{\text{simple}})$. If we let $C = (\mathscr{F}(\mathscr{B}_0^{\text{simple}}))^{-1}$, then the shape function for the DOF on face i (i.e., $\mathscr{F}(\phi_{0,i}^{\text{simple}}) = \mathbf{e}_{i+1}^T$) is

$$\phi_{0,i}^{\text{simple}}(\mathbf{x}) = C_{i,1}(\mathbf{x} - \mathbf{x}_{124}) + C_{i,2}(\mathbf{x} - \mathbf{x}_{034}) + C_{i,3}(\mathbf{x} - \mathbf{x}_{025})$$
$$+ C_{i,4}(\mathbf{x} - \mathbf{x}_{024}) + C_{i,5}\sigma_{0,0}^{1,3} + C_{i,6}\sigma_{0,0}^{3,5}. \tag{35}$$

In fact, an explicit basis can be constructed without the need to invert a matrix. Recall that for any point $\mathbf{x}$ on face 1, $(\mathbf{x} - \mathbf{x}_{024}) \cdot v_1$ denotes the distance from point $\mathbf{x}_{024}$ to face 1, which is a constant. Compute the numbers

$$\alpha = (\mathbf{x} - \mathbf{x}_{024}) \cdot v_1|_{f_1}, \quad \beta = (\mathbf{x} - \mathbf{x}_{024}) \cdot v_3|_{f_3}, \quad \text{and} \quad \gamma = (\mathbf{x} - \mathbf{x}_{024}) \cdot v_5|_{f_5},$$

which are positive due to the convexity of E, and then $\mathscr{F}_{024}(\mathbf{x} - \mathbf{x}_{024}, \sigma_{0,0}^{1,3}, \sigma_{0,0}^{3,5})$ vanishes and

$$\mathscr{F}_{135}(\mathbf{x} - \mathbf{x}_{024}, \sigma_{0,0}^{1,3}, \sigma_{0,0}^{3,5}) = \begin{bmatrix} \alpha & \beta & \gamma \\ 1/|f_1| & -1/|f_3| & 0 \\ 0 & 1/|f_3| & -1/|f_5| \end{bmatrix}. \tag{36}$$

Guided by these fluxes, we construct the following linear combinations:

$$\phi_{0,1}^{\text{simple}}(\mathbf{x}) = |f_1| \frac{\mathbf{x} - \mathbf{x}_{024} + (|f_3|\beta + |f_5|\gamma)\sigma_{0,0}^{1,3} + |f_5|\gamma\sigma_{0,0}^{3,5}}{|f_1|\alpha + |f_3|\beta + |f_5|\gamma}, \tag{37}$$

$$\phi_{0,3}^{\text{simple}}(\mathbf{x}) = |f_3| \frac{\mathbf{x} - \mathbf{x}_{024} - |f_1|\alpha\sigma_{0,0}^{1,3} + |f_5|\gamma\sigma_{0,0}^{3,5}}{|f_1|\alpha + |f_3|\beta + |f_5|\gamma}, \tag{38}$$

$$\phi_{0,5}^{\text{simple}}(\mathbf{x}) = |f_5| \frac{\mathbf{x} - \mathbf{x}_{024} - |f_1|\alpha\sigma_{0,0}^{1,3} - (|f_1|\alpha + |f_3|\beta)\sigma_{0,0}^{3,5}}{|f_1|\alpha + |f_3|\beta + |f_5|\gamma}. \tag{39}$$

Using (36), inspection shows that indeed $\mathscr{F}(\phi_{0,i}^{\text{simple}}) = \mathbf{e}_{i+1}^T$, $i = 1, 3, 5$. From these functions, we then construct

$$\phi_{0,0}^{\text{simple}}(\mathbf{x}) = \frac{v_2 \times v_4 - (v_2 \times v_4) \cdot (v_1\phi_{0,1}^{\text{simple}} + v_3\phi_{0,3}^{\text{simple}} + v_5\phi_{0,5}^{\text{simple}})}{(v_2 \times v_4) \cdot v_0}, \tag{40}$$

$$\phi_{0,2}^{\text{simple}}(\mathbf{x}) = \frac{v_0 \times v_4 - (v_0 \times v_4) \cdot (v_1\phi_{0,1}^{\text{simple}} + v_3\phi_{0,3}^{\text{simple}} + v_5\phi_{0,5}^{\text{simple}})}{(v_0 \times v_4) \cdot v_2}, \tag{41}$$

$$\phi_{0,4}^{\text{simple}}(\mathbf{x}) = \frac{v_0 \times v_2 - (v_0 \times v_2) \cdot (v_1\phi_{0,1}^{\text{simple}} + v_3\phi_{0,3}^{\text{simple}} + v_5\phi_{0,5}^{\text{simple}})}{(v_0 \times v_2) \cdot v_4}. \tag{42}$$

Using the property $\mathscr{F}(\phi_{0,i}^{\text{simple}}) = \mathbf{e}_{i+1}^T$, $i = 1,3,5$, already established, a careful inspection of (40)–(42) shows that these functions also satisfy the required property $\mathscr{F}(\phi_{0,i}^{\text{simple}}) = \mathbf{e}_{i+1}^T$, $i = 0,2,4$. Therefore, we have constructed a simple set of shape functions for the lowest order case $r = 0$.

5.1.2 A more general supplemental space for $r = 0$

While $\mathscr{B}_0^{\text{simple}}$ is well defined and simple to implement, it is defined in a highly non-symmetric way. One could average over all similar constructions, but it is not clear how to weight them. An alternative is to add supplements that are as different as possible from the polynomial part $\mathbb{P}_0^3 \oplus \mathbf{x}\mathbb{P}_0$, and subject to the divergence-free constraint. A criterion is to consider the fluxes generated by this part, and take supplements with fluxes that span the orthogonal complement. We denote the flux matrix for $\mathscr{B}_0^{\text{poly}}$ as

$$
M = \left[\mathscr{F}_{024}(\mathscr{B}_0^{\text{poly}}) \; \mathscr{F}_{135}(\mathscr{B}_0^{\text{poly}}) \right] = \begin{bmatrix} a_1 & 0 & 0 & 0 & b_1 & c_1 \\ 0 & b_2 & 0 & a_2 & 0 & c_2 \\ 0 & 0 & c_3 & a_3 & b_3 & 0 \\ 0 & 0 & 0 & \alpha & \beta & \gamma \end{bmatrix}, \tag{43}
$$

where each letter (a_i, b_i, c_i, α, β, and γ) stands for a specific positive number. The orthogonal complement of the row space of M is easily seen to be spanned by N^T (i.e., $\operatorname{rank} M = 4$, $\operatorname{rank} N = 2$ and $MN^T = 0$), where

$$
N = \begin{bmatrix} \alpha b_1/a_1 & -\beta a_2/b_2 & (\alpha b_3 - \beta a_3)/c_3 & \beta & -\alpha & 0 \\ (\beta c_1 - \gamma b_1)/a_1 & \beta c_2/b_2 & -\gamma b_3/c_3 & 0 & \gamma & -\beta \end{bmatrix}. \tag{44}
$$

Let S denote the 2×6 matrix with rows being the desired supplemental fluxes. The divergence-free constraint can be written as $S\varphi = 0$ in terms of the vector of face areas, which is

$$
\varphi = \left(|f_0|, |f_1|, |f_2|, |f_3|, |f_4|, |f_5| \right). \tag{45}
$$

We define S to be the projection of N to the orthogonal complement of $\operatorname{span}\{\varphi\}$, i.e.,

$$
S = N\left(I - \frac{\varphi\varphi^T}{\varphi^T \varphi} \right), \tag{46}
$$

and then we define $\mathbb{S}_0 = \operatorname{span}\{\sigma_{0,0}^1, \sigma_{0,0}^2\}$, where

$$
\sigma_{0,0}^1 = \mathscr{P}_E\left(S_{1,1}\hat{\sigma}_{0,0}^0 + S_{1,2}\hat{\sigma}_{0,0}^1 + S_{1,3}\hat{\sigma}_{0,0}^2 + S_{1,4}\hat{\sigma}_{0,0}^3 + S_{1,5}\hat{\sigma}_{0,0}^4 + S_{1,6}\hat{\sigma}_{0,0}^5 \right), \tag{47}
$$

$$
\sigma_{0,0}^2 = \mathscr{P}_E\left(S_{2,1}\hat{\sigma}_{0,0}^0 + S_{2,2}\hat{\sigma}_{0,0}^1 + S_{2,3}\hat{\sigma}_{0,0}^2 + S_{2,4}\hat{\sigma}_{0,0}^3 + S_{2,5}\hat{\sigma}_{0,0}^4 + S_{2,6}\hat{\sigma}_{0,0}^5 \right), \tag{48}
$$

since, by (26) and (12)–(13), these supplements satisfy the constraint of being divergence-free and produce the desired fluxes S on each face.

It remains to verify that the DOFs are independent after applying the projection. To this end, we note that φ is not in the span of the rows of N. This is true since $M\varphi \neq 0$ (at least one row of M represents a function with a nonzero divergence), which implies that $\varphi \notin (M^T)^\perp = \operatorname{row}(N)$. Independence of the DOFs is a consequence of the following, more general lemma.

Lemma 1 *Suppose that M is $m \times (m+n)$, N is $n \times (m+n)$, and $\begin{bmatrix} M \\ N \end{bmatrix}$ is invertible. Let φ be an $(m+n)$-vector that does not lie in the row space of N. Let the projection $P_\varphi = \frac{\varphi \varphi^T}{\varphi^T \varphi}$. If $S = N(I - P_\varphi)$, then $\begin{bmatrix} M \\ S \end{bmatrix}$ is invertible.*

Proof By a change of basis, we may assume that $M = \begin{bmatrix} I_m & 0 \end{bmatrix}$ and $N = \begin{bmatrix} 0 & I_n \end{bmatrix}$. Normalize and partition $\varphi = \begin{pmatrix} \mathbf{a} \\ \mathbf{b} \end{pmatrix}$ into m- and n-subvectors. Now the projection in block form is

$$P_\varphi = \begin{bmatrix} \mathbf{a}\mathbf{a}^T & \mathbf{a}\mathbf{b}^T \\ \mathbf{b}\mathbf{a}^T & \mathbf{b}\mathbf{b}^T \end{bmatrix},$$

and $S = \begin{bmatrix} -\mathbf{b}\mathbf{a}^T & I_n - \mathbf{b}\mathbf{b}^T \end{bmatrix}$. Since $\|\mathbf{b}\mathbf{b}^T\| < 1$ (recall $\mathbf{a} \neq 0$), we conclude that $I_n - \mathbf{b}\mathbf{b}^T$ is invertible, and thus also $\begin{bmatrix} I_m & 0 \\ -\mathbf{b}\mathbf{a}^T & I_n - \mathbf{b}\mathbf{b}^T \end{bmatrix} = \begin{bmatrix} M \\ S \end{bmatrix}$. $\qquad \square$

5.2 The case $r = 1$

We concentrate on the reduced space $\mathbf{V}_1^{\mathrm{red}}(E) = \mathbb{P}_1^3 \oplus \mathbb{S}_1$, since we merely add $\mathbf{x}\tilde{\mathbb{P}}_1$ to define $\mathbf{V}_1(E)$. The divergence of $\mathbf{V}_1^{\mathrm{red}}(E)$ is constant as in the case $r = 0$, but now the normal face fluxes are linear, so there are 18 of them in total. Since $\dim \mathbb{P}_1^3 = 12$, we need 6 supplements.

Please recall the notation from Fig. 1. We can view the hexahedron as containing a tetrahedron nestled in the corner near $\mathbf{x}_{024}$, i.e., the tetrahedron with the four vertices $\mathbf{x}_{024}$, $\mathbf{x}_{124}$, $\mathbf{x}_{034}$, and $\mathbf{x}_{025}$. The usual BDM (i.e., BDDF) space on tetrahedra [7] is $\mathbb{P}_1^3$, so we know that we can set the fluxes independently on the faces 0, 2, and 4 by polynomial vector functions (since these fluxes are independent degrees of freedom for the tetrahedral element $\mathbb{P}_1^3 \subset \mathbf{V}_1^{\mathrm{red}}(E)$). To find these functions, we first define the six linear functions

$$\lambda_i(\mathbf{x}) = -(\mathbf{x} - \mathbf{x}_i) \cdot v_i, \quad i = 0, 1, \ldots, 5, \tag{49}$$

and the linear function associated with the plane f_6 through $\mathbf{x}_{124}$, $\mathbf{x}_{034}$, and $\mathbf{x}_{025}$,

$$\lambda_6(\mathbf{x}) = -(\mathbf{x} - \mathbf{x}_6) \cdot v_6, \tag{50}$$

where $\mathbf{x}_6$ lies on f_6 and v_6 is the unit normal pointing *into* the tetrahedron.

Since $\nabla \lambda_i = -v_i$, we have that

$$\nabla \times (\lambda_i \lambda_j v_k) = -\lambda_i v_j \times v_k - \lambda_j v_i \times v_k,$$

which has no normal flux on faces i, j, and k. As we show below, we can independently set the 9 fluxes on the faces 0, 2, and 4, respectively, by the functions

$$\psi_0 = \mathbf{x} - \mathbf{x}_{124}, \quad \psi_1 = \nabla \times (\lambda_2 \lambda_6 v_4), \quad \psi_2 = \nabla \times (\lambda_4 \lambda_6 v_2), \tag{51}$$

$$\psi_3 = \mathbf{x} - \mathbf{x}_{034}, \quad \psi_4 = \nabla \times (\lambda_0 \lambda_6 v_4), \quad \psi_5 = \nabla \times (\lambda_4 \lambda_6 v_0), \tag{52}$$

$$\psi_6 = \mathbf{x} - \mathbf{x}_{025}, \quad \psi_7 = \nabla \times (\lambda_0 \lambda_6 v_2), \quad \psi_8 = \nabla \times (\lambda_2 \lambda_6 v_0). \tag{53}$$

The rest of the polynomial space is associated to f_6, and consists of the functions

$$\psi_9 = \mathbf{x} - \mathbf{x}_{024}, \quad \psi_{10} = \nabla \times (\lambda_0 \lambda_2 v_4), \quad \psi_{11} = \nabla \times (\lambda_2 \lambda_4 v_0). \tag{54}$$

It is convenient for the discussion to map E to a simpler shape $\tilde{E}$ using an affine map. In the case of an affine map, no polynomial spaces are changed, so conclusions about fluxes on $\partial \tilde{E}$ hold for ∂E. We take $\tilde{E}$ as in Fig. 1, but it is the result of a translation that makes $\mathbf{x}_{024} = 0$. Rotations, dilations, and shear maps can then make $\mathbf{x}_{124} = \mathbf{e}_1$, $\mathbf{x}_{034} = \mathbf{e}_2$, and $\mathbf{x}_{025} = \mathbf{e}_3$. We proceed as if $E = \tilde{E}$. Then

$$v_0 = -\mathbf{e}_1, \quad v_2 = -\mathbf{e}_2, \quad v_4 = -\mathbf{e}_3, \quad v_6 = -(\mathbf{e}_1 + \mathbf{e}_2 + \mathbf{e}_3)/\sqrt{3},$$
$$\lambda_0 = x_1, \quad \lambda_2 = x_2, \quad \lambda_4 = x_3, \quad \lambda_6 = (x_1 + x_2 + x_3 - 1)/\sqrt{3}.$$

Thus, for face 0,

$$\psi_0 = \begin{pmatrix} x_1 - 1 \\ x_2 \\ x_3 \end{pmatrix}, \quad \psi_1 = \frac{1}{\sqrt{3}} \begin{pmatrix} 1 - x_1 - 2x_2 - x_3 \\ x_2 \\ 0 \end{pmatrix}, \quad \psi_2 = \frac{1}{\sqrt{3}} \begin{pmatrix} x_1 + x_2 + 2x_3 - 1 \\ 0 \\ -x_3 \end{pmatrix}, \tag{55}$$

and so we compute the columns of $\mathscr{F}$ for faces 0, 2, and 4 as

$$\mathscr{F}_{024}(\psi_0, \psi_1, \psi_2) = \begin{bmatrix} 1 & 0 & 0 \\ 2x_2 + x_3 - 1 & 0 & 0 \\ 1 - x_2 - 2x_3 & 0 & 0 \end{bmatrix}. \tag{56}$$

The other two triples, (ψ_3, ψ_4, ψ_5) for face 2 and (ψ_6, ψ_7, ψ_8) for face 4, are similar, so we conclude that indeed these 9 functions independently set the 9 fluxes on the faces 0, 2, and 4.

For the other three faces 1, 3, and 5, we have that

$$\psi_9 = \begin{pmatrix} x_1 \\ x_2 \\ x_3 \end{pmatrix}, \quad \psi_{10} = \begin{pmatrix} -x_1 \\ x_2 \\ 0 \end{pmatrix}, \quad \psi_{11} = \begin{pmatrix} 0 \\ -x_2 \\ x_3 \end{pmatrix}. \tag{57}$$

Note that these three functions have no normal flux on faces 0, 2, and 4. In the following discussion, for simplicity, we replace ψ_9, ψ_{10}, and ψ_{11} with ψ_9^*, ψ_{10}^*, and ψ_{11}^* where

$$\psi_9^* = \begin{pmatrix} x_1 \\ 0 \\ 0 \end{pmatrix}, \quad \psi_{10}^* = \begin{pmatrix} 0 \\ x_2 \\ 0 \end{pmatrix}, \quad \psi_{11}^* = \begin{pmatrix} 0 \\ 0 \\ x_3 \end{pmatrix}. \tag{58}$$

We can do this because

$$\frac{1}{3} \begin{pmatrix} x_1 & -x_1 & 0 \\ x_2 & x_2 & -x_2 \\ x_3 & 0 & x_3 \end{pmatrix} \begin{pmatrix} 1 & 1 & 1 \\ -2 & 1 & 1 \\ -1 & -1 & 2 \end{pmatrix} = \begin{pmatrix} x_1 & 0 & 0 \\ 0 & x_2 & 0 \\ 0 & 0 & x_3 \end{pmatrix}, \tag{59}$$

and the transformation matrix is invertible, so ψ_9, ψ_{10}, and ψ_{11} span the same space as ψ_9^*, ψ_{10}^*, and ψ_{11}^*. Therefore,

$$\mathscr{F}_{135}(\psi_9^*, \psi_{10}^*, \psi_{11}^*) = \begin{bmatrix} x_1 v_{1,1} & x_1 v_{3,1} & x_1 v_{5,1} \\ x_2 v_{1,2} & x_2 v_{3,2} & x_2 v_{5,2} \\ x_3 v_{1,3} & x_3 v_{3,3} & x_3 v_{5,3} \end{bmatrix}. \tag{60}$$

We must add supplements to the set $\{\psi_9^*, \psi_{10}^*, \psi_{11}^*\}$ that also have no normal flux on faces 0, 2, and 4. Moreover, the normal fluxes of the supplements on the remaining three faces, when combined with (60), must independently span the spaces of linear polynomials. There are at least two ways to choose the supplements, a non-symmetric way and a symmetric way.

Theorem 1 (Non-Symmetric supplements) *There exist constants s and t such that if the supplemental functions σ_0 to σ_3, σ_4^*, and σ_5^* are defined to take the fluxes*

$$\mathscr{F}_{135}(\sigma_0, \sigma_1, \sigma_2, \sigma_3, \sigma_4^*, \sigma_5^*) = \begin{bmatrix} x_2 - c_2^1 & 0 & 0 \\ x_3 - c_3^1 & 0 & 0 \\ 0 & x_1 - c_1^3 & 0 \\ 0 & x_3 - c_3^3 & 0 \\ (-|f_5|c_1^5 + t)/|f_1| & -t/|f_3| & x_1 \\ -s/|f_1| & (-|f_5|c_2^5 + s)/|f_3| & x_2 \end{bmatrix}, \quad (61)$$

where the constant c_ℓ^i is the average over face i of the variable x_ℓ, then they provide independent flux degrees of freedom.

Theorem 2 (Symmetric supplements) *Let the supplemental functions σ_0 to σ_5 take the fluxes*

$$\mathscr{F}_{135}(\sigma_0, \sigma_1, \sigma_2, \sigma_3, \sigma_4, \sigma_5) = \begin{bmatrix} x_2 - c_2^1 & 0 & 0 \\ x_3 - c_3^1 & 0 & 0 \\ 0 & x_1 - c_1^3 & 0 \\ 0 & x_3 - c_3^3 & 0 \\ 0 & 0 & x_1 - c_1^5 \\ 0 & 0 & x_2 - c_2^5 \end{bmatrix}, \quad (62)$$

where the constant c_ℓ^i is the average over face i of the variable x_ℓ. These provide independent flux degree of freedoms as long as the matrix

$$\mathbf{C} \circ \mathbf{H} = \begin{bmatrix} c_1^1 v_{1,1} & c_1^3 v_{3,1} & c_1^5 v_{5,1} \\ c_2^1 v_{1,2} & c_2^3 v_{3,2} & c_2^5 v_{5,2} \\ c_3^1 v_{1,3} & c_3^3 v_{3,3} & c_3^5 v_{5,3} \end{bmatrix} \quad (63)$$

is invertible.

   The proofs of Theorems 1 and 2 appear in Appendices C and B, respectively. The invertibility of matrix $\mathbf{C} \circ \mathbf{H}$ in (63) is discussed in Appendix A. We remark that we have not seen a perturbed hexahedron in practice that violates the invertibility condition. In Appendix A, we prove the invertibility condition (63), i.e., Theorem 3 below, in two special cases: hexahedra with at least one pair of faces being parallel and truncated pillars.

Definition 1 A cuboidal hexahedron E is a truncated pillar if four of its twelve edges are parallel. These four edges form the pillar. If they are extended to infinity, the other two faces of E are formed by truncating the pillar.

Theorem 3 *If E is a cuboidal hexahedron that either has two pair of faces being parallel or is a truncated pillar, then* (63) *holds.*

Meshes of cuboidal hexahedra with at least one pair of faces being parallel are used in many applications. For any cuboidal hexahedron E with flat faces, it is easy to check this condition without transformation to $\tilde{E}$. For example, the mesh $\mathscr{T}_h^2$ in Section 6 satisfies this condition.

Meshes of truncated pillars are widely used. For example, in reservoir simulation and geological modeling, it is very common that the dataset is given in the corner-point grid format [15]. The grid format gives a set of pillar lines which run from the top to the bottom of the model and, in many cases, the lines are vertical. The mesh $\mathscr{T}_h^3$ in Section 6 is an example of a grid made by truncated vertical pillars.

The vector functions providing the fluxes we require in (61) and (62) can be easily obtained using the functions $\sigma_{\ell,m}^1$ (22) and $\sigma_{0,0}^{i,j}$ (28) defined in Section 4. For example, σ_0 here is exactly $\sigma_{1,0}^1$ of (22), and

$$
\begin{aligned}
\mathscr{F}_{135}(\sigma_4^*) &= \left[(-|f_5|c_1^5 + t)/|f_1| \quad -t/|f_3| \quad x_1 \right] \\
&= \left[0 \quad 0 \quad x_1 - c_1^5 \right] + |f_5|c_1^5 \left[-\frac{1}{|f_1|} \quad 0 \quad \frac{1}{|f_5|} \right] + t \left[\frac{1}{|f_1|} \quad -\frac{1}{|f_3|} \quad 0 \right] \\
&= \mathscr{F}_{135}\left(\sigma_{1,0}^5 \right) + |f_5|c_1^5 \mathscr{F}_{135}\left(\sigma_{0,0}^{5,1} \right) + t \mathscr{F}_{135}\left(\sigma_{0,0}^{1,3} \right),
\end{aligned}
$$

so $\sigma_4^* = \sigma_{1,0}^5 + |f_5|c_1^5 \sigma_{0,0}^{5,1} + t \sigma_{0,0}^{1,3}$.

In conclusion, if we know that $\mathbf{C} \circ \mathbf{H}$ is invertible for the meshes used, we can apply the symmetric supplements. On the other hand, one can always take the non-symmetric supplements for any mesh, provided s and t are chosen properly. A general method for handling $r = 1$ is contained in the next subsection.

5.3 The general case $r \geq 1$

In general, the DOFs of our mixed finite element spaces are allocated as

$$
\begin{aligned}
\mathbf{V}_r(E) &= \mathbb{P}_r^3 \oplus \mathbf{x}\tilde{\mathbb{P}}_r \oplus \mathbb{S}_r = \mathbb{E}_r \oplus \mathbb{D}_r \oplus \mathbb{B}_r \\
\text{or} \quad \mathbf{V}_r^{\text{red}}(E) &= \mathbb{P}_r^3 \oplus \mathbb{S}_r \qquad = \mathbb{E}_r \oplus \mathbb{D}_r^{\text{red}} \oplus \mathbb{B}_r.
\end{aligned}
\tag{64}
$$

Here $\mathbb{E}_r$ are the functions that have constant divergence and independently cover the normal flux DOFs (8). The functions in $\mathbb{D}_r$ or $\mathbb{D}_r^{\text{red}}$ match the (nonconstant) divergence DOFs (7). One of these functions can be constructed from a basis function in $\mathbf{x}\tilde{\mathbb{P}}_r^*$ or $\mathbf{x}\tilde{\mathbb{P}}_{r-1}^*$, respectively, but then modified by the functions in $\mathbb{E}_r$ to remove the face normal fluxes. Finally, the divergence-free bubbles $\mathbb{B}_r$ are left over, and provide the final set of DOFs. Since $\mathbb{P}_r^3 = \text{curl}\,\mathbb{P}_{r+1}^3 \oplus \mathbf{x}\mathbb{P}_{r-1}$, we conclude that

$$
\mathbb{E}_r \oplus \mathbb{B}_r = \text{curl}\,\mathbb{P}_{r+1}^3 \oplus \mathbf{x}\mathbb{P}_0 \oplus \mathbb{S}_r.
\tag{65}
$$

Thus, our task is to construct the supplemental space $\mathbb{S}_r$ of functions with zero divergence so that the normal flux DOFs (8) in $\text{curl}\,\mathbb{P}_{r+1}^3 \oplus \mathbf{x}\mathbb{P}_0 \oplus \mathbb{S}_r$ are independent.

Cockburn and Fu [10] determined the minimal number of supplemental functions (which they call "filling functions") needed to produce the space $\mathbb{E}_r$ on various elements, including a cuboidal hexahedron. In particular, [10, Lemma 4.6 and Theorems 2.10–2.15] identify the fluxes required (but note that they label the faces counting from 1 rather than 0). Their construction is to obtain supplements that have no flux on faces 0, 1, and 2. They specify the needed fluxes on face 3, but allow any flux on the last two faces. They then specify the needed fluxes on face 4, but again allow any flux on the last face. Finally, face 5 has a set of required fluxes, and these can be matched by divergence-free functions. As mentioned previously, Cockburn and Fu use a mesh of tetrahedral elements within the hexahedron to construct their supplemental functions. We can instead use the ideas of Sections 3–4.

The number of additional fluxes (see [10, Cor. 4.5 and Table 4]) is bounded by $3(r+1)$ and depends on the geometry, in particular, on the number of parallel faces. The cube requires $3(r+1)$ supplemental functions. It is numerically delicate to vary the number of supplemental functions based on the number of parallel sides, since an element E may have almost, but not quite, parallel faces.

A numerically safe way to proceed is to use the general construction of Subsection 5.1.2. Since it is difficult to characterize what functions lie in $\mathbb{B}_r$ (see, however, [10]), we simply compute the flux matrix of the entire polynomial part of the space, i.e., of a basis for $\operatorname{curl}\mathbb{P}_{r+1}^3 \oplus \mathbf{x}\mathbb{P}_0$, which has dimension $n = \dim\mathbb{P}_r^3 - \dim(\mathbf{x}\mathbb{P}_{r-1}^*) = \frac{1}{6}(r+2)(r+1)(2r+9)+1$. To proceed, it is convenient to express the flux matrix as an ordinary matrix of numbers, so we expand every normal flux polynomial in a basis that includes 1 and everything orthogonal to 1. A simple choice is displayed in (22) for face 1, i.e., take 1 and the functions $x_{i_1}^\ell x_{j_1}^m - c_{\ell,m}^1$ for $1 \le \ell+m \le r$. The expansion coefficients give the matrix M^{full}, which is $n \times 3(r+2)(r+1)$.

We reduce the number of rows in M^{full} to M by including only a basis for the row space. This removes the interior bubble parts of the space. It may be better to compute the singular values of M^{full} and remove all rows corresponding to small singular values. In fact, we suggest reducing M^{full} to an $n - 3(r+1)$ matrix, so that $3(r+1)$ supplements are needed, regardless of the geometry. This may create more interior bubble functions than is necessary, but it safely handles any geometry.

We proceed to find a basis N^T of $(M^T)^\perp$. Let the area vector φ be analogous to the one defined in (45) (it is the same, except that it has more zeros). The desired supplemental fluxes S are then defined by the formula in (46), i.e., $S = N\left(I - \dfrac{\varphi\varphi^T}{\varphi^T\varphi}\right)$. We construct supplemental functions $\mathbb{S}_r$ having these fluxes. By Lemma 1, these fluxes are independent of the ones from M, and so the space $\mathbb{E}_r$ is well-defined. Any extra functions are divergence-free bubbles, which can be modified to have no face fluxes.

In the hybrid form of the mixed method [5], the Lagrange multiplier space on the face f is simply $\mathbb{P}_r(f)$, and implementation is clear up to evaluation of the integrals over the elements. If the hybrid form is not used, one needs $H(\operatorname{div})$-conforming finite element shape functions to form a local basis. This is done by inverting the numerical counterpart of the local flux matrix, as discussed in (35) for $r = 0$.

5.4 Construction of the π operator

Once the spaces $\mathbb{E}_r$, $\mathbb{D}_r$ or $\mathbb{D}_r^{\text{red}}$, and $\mathbb{B}_r$ have been determined, one can define the Raviart-Thomas [16] or Fortin [9] projection operator π_r onto $\mathbf{V}_r(E) = \mathbb{E}_r \oplus \mathbb{D}_r \oplus \mathbb{B}_r$ or π_r^{red} onto $\mathbf{V}_r^{\text{red}}(E) = \mathbb{E}_r \oplus \mathbb{D}_r^{\text{red}} \oplus \mathbb{B}_r$. One simply matches the DOFs (7)–(8) to fix the part in $\mathbb{E} \oplus \mathbb{D}_r$ or $\mathbb{E} \oplus \mathbb{D}_r^{\text{red}}$. To these DOFs, we add

$$(\mathbf{v}, \psi)_E \quad \forall \psi \in \mathbb{B}_r. \tag{66}$$

Because of (7), these projection operators satisfy the commuting diagram property, namely, that

$$\nabla \cdot \pi_r \mathbf{v} = \mathscr{P}_{W_r} \nabla \cdot \mathbf{v} \quad \text{and} \quad \nabla \cdot \pi_r^{\text{red}} \mathbf{v} = \mathscr{P}_{W_{r-1}} \nabla \cdot \mathbf{v}, \tag{67}$$

where $\mathscr{P}_{W_s}$ is the L^2-projection onto W_s. Moreover, since our spaces contain full sets of polynomials, $\mathbf{V}_r \times W_r$ will have full $H(\text{div})$-approximation properties and $\mathbf{V}_r^{\text{red}} \times W_{r-1}$ will have reduced $H(\text{div})$-approximation properties. Moreover, we have the following result.

Lemma 2 *Assume that the computational mesh is shape-regular. The spaces $\mathbf{V}_r \times W_r$ and $\mathbf{V}_r^{\text{red}} \times W_{r-1}$ satisfy the inf-sup conditions*

$$\inf_{w \, \in \, W_r} \sup_{\mathbf{v} \in \mathbf{V}_r} \frac{(\nabla \cdot \mathbf{v}, w)_\Omega}{\|\mathbf{v}\|_\mathbf{V} \|w\|_W} \geq \gamma > 0 \quad \text{and} \quad \inf_{w \, \in \, W_{r-1}} \sup_{\mathbf{v} \in \mathbf{V}_r^{\text{red}}} \frac{(\nabla \cdot \mathbf{v}, w)_\Omega}{\|\mathbf{v}\|_\mathbf{V} \|w\|_W} \geq \gamma > 0. \tag{68}$$

Moreover, if $\mathbf{u}$ is sufficiently smooth and h is the diameter of the computational mesh, then

$$\|\mathbf{u} - \pi_r \mathbf{u}\| + \|\mathbf{u} - \pi_r^{\text{red}} \mathbf{u}\| \leq Ch^{s+1} \|\mathbf{u}\|_{s+1}, \qquad 1 \leq s \leq r, \tag{69}$$

$$\|\nabla \cdot (\mathbf{u} - \pi_r \mathbf{u})\| \leq Ch^{s+1} \|\nabla \cdot \mathbf{u}\|_{s+1}, \quad 1 \leq s \leq r, \tag{70}$$

$$\|\nabla \cdot (\mathbf{u} - \pi_r^{\text{red}} \mathbf{u})\| \leq Ch^{s+1} \|\nabla \cdot \mathbf{u}\|_{s+1}, \quad 1 \leq s \leq r-1. \tag{71}$$

The condition for a computational mesh to be shape regular is that each element E is uniformly shape-regular [13, pp. 104–105], which means that E contains fifteen (overlapping) simplices constructed from any choice of four vertices, and each such simplex has an inscribed ball, the minimal radius of which is ρ_E. If h_E denotes the diameter of E, the requirement is that the ratio $\rho_E/h_E \geq \sigma_* > 0$, where σ_* is independent of the meshes as $h \to 0$ ($h = \max_E h_E$).

The proof of Lemma 2 is quite standard and classic in the mixed finite element literature (e.g., see [16,7,9], or see the proof outlined in [1, Section 2] for the two families of similar elements defined on quadrilaterals).

6 Some numerical results

In this section we present convergence studies for various low order mixed spaces. We include the new full and reduced spaces defined in Section 5, which we will designate as AT spaces to avoid confusion. The AT_0 space used is the simple one given in (33)
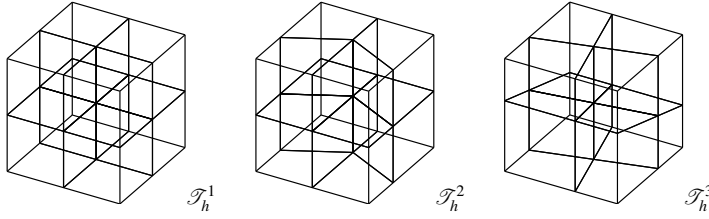
Fig. 2 Mesh of $2 \times 2 \times 2$ cubes for the three base meshes. Finer meshes are constructed by repeating this base mesh pattern over the domain, appropriately reflected to maintain mesh conformity. Note that the meshes have 3, 2, and 0 pairs of parallel faces per element, respectively.

(or, equivalently, (37)–(42)). The AT_1 full and reduced spaces used are constructed using the symmetric supplemental fluxes of (62) since the invertibility of $\mathbf{C} \circ \mathbf{H}$ is known for $\mathscr{T}_h^2$ and $\mathscr{T}_h^3$ (see Theorem 3).

The performance of the AT spaces will be compared to RT, BDDF, and ABF spaces. For the 3-D ABF space, we use the optimal space $\hat{\mathscr{P}}_r^{\text{opt}}(\hat{K})$ of Bergot and Durufle [6]. The test problem is defined on the unit cube $\Omega = [0,1]^3$ with the coefficient $a = 1$ and the source function $f(\mathbf{x}) = 3\pi^2 \cos(\pi x_1) \cos(\pi x_2) \cos(\pi x_3)$. The exact solution is

$$p(x_1, x_2, x_3) = \cos(\pi x_1)\cos(\pi x_2)\cos(\pi x_3), \tag{72}$$

$$\mathbf{u}(x_1, x_2, x_3) = \pi \begin{pmatrix} \sin(\pi x_1)\cos(\pi x_2)\cos(\pi x_3) \\ \cos(\pi x_1)\sin(\pi x_2)\cos(\pi x_3) \\ \cos(\pi x_1)\cos(\pi x_2)\sin(\pi x_3) \end{pmatrix}. \tag{73}$$

In the computations, we apply the hybrid form of the mixed finite element method [5]. Let $\mathscr{T}_h$ be the finite element partition of the domain Ω. For the mixed spaces $\mathbf{V}_h \times W_h$, let $\mathbf{V}_h^*$ agree with $\mathbf{V}_h$ on each element $E \in \mathscr{T}_h$, but relax the condition that the normal flux be continuous on the faces of the elements. The hybrid method is: Find $\mathbf{u}_h \in \mathbf{V}_h^*$, $p_h \in W_h$, and $\hat{p}_h \in M_h$ such that

$$(a^{-1}\mathbf{u}_h, \mathbf{v})_E - (p_h, \nabla \cdot \mathbf{v})_E + (\hat{p}_h, \mathbf{v} \cdot \nu_i)_{\partial E} = 0 \qquad \forall \mathbf{v} \in \mathbf{V}_h(E), E \in \mathscr{T}_h, \tag{74}$$

$$\sum_{E \in \mathscr{T}_h} (\nabla \cdot \mathbf{u}_h, w)_E = (f, w)_\Omega \quad \forall w \in W_h, \tag{75}$$

$$\sum_{E \in \mathscr{T}_h} (\mathbf{u}_h \cdot \nu, \mu)_{\partial E \setminus \partial \Omega} = 0 \qquad \forall \mu \in M_h. \tag{76}$$

The Lagrange multiplier or trace finite element space M_h is defined locally by $M_h|_f = M_h(f) = \mathbf{V}_h \cdot \nu|_f$ for each face f of the computational mesh. For the AT spaces, $M_r(f) = \mathbb{P}_r(f)$. We require that the L^2-projection of the Dirichlet boundary condition be imposed on $\hat{p}_h$.

Solutions are computed on three different sequences of meshes. The first sequence, $\mathscr{T}_h^1$, is a uniform mesh of n^3 cubes (three sets of parallel faces per element). The second sequence, $\mathscr{T}_h^2$, is obtained from the 2-D trapezoidal meshes used in Arnold, Boffi, and Falk [4] by simply lifting them in the third direction. These elements have two pair of parallel faces per element. The third sequence of meshes, $\mathscr{T}_h^3$,

Table 1 A comparison of the dimensions of the local RT, ABF, and AT spaces on a hexahedron E. Only the ABF and AT spaces give optimal order convergence on hexahedra.

	RT$_r$	ABF$_r$	AT$_r$
dim$\mathbf{V}(E)$	$3(r+2)(r+1)^2$	$3(r+4)(r+2)^2$	$\frac{1}{2}(r+1)(r+2)(r+4)$ $+3(r+1)$ ($+2$ if $r=0$)
dim$W(E)$	$(r+1)^3$	$(r+2)^3+3(r+2)^2$	$\frac{1}{6}(r+1)(r+2)(r+3)$
$r=0$	$6+1$	$48+20$	$6+1$
$r=1$	$36+8$	$135+54$	$21+4$

is chosen so as to have no pair of faces being parallel. The first $2 \times 2 \times 2$ mesh for each sequence is shown in Fig. 2. Finer meshes are constructed by repeating this sub-mesh pattern over the domain, appropriately reflected to maintain mesh conformity.

The cubical mesh $\mathscr{T}_h^1$ provides a reference on which all the mixed methods work well. It turns out that the second and third meshes provide similar results, so we show only results for the most irregular case of the third mesh $\mathscr{T}_h^3$.

6.1 Full $H(\mathrm{div})$-approximation spaces

The local number of DOFs for each full $H(\mathrm{div})$-approximation finite element space can be found in Table 1. Note that according to Bergot and Durufle [6], the optimal ABF$_0$ space should satisfy the property $\mathscr{P}_E(\hat{\mathbf{V}}_{\mathrm{ABF}}^0(E)) \supset \mathbb{P}_0^3 \oplus \mathbf{x}\mathbb{P}_0$, and so it is defined to be $\hat{\mathbf{V}}_{\mathrm{ABF}}^0(E) = \mathbb{P}_{3,1,1} \times \mathbb{P}_{1,3,1} \times \mathbb{P}_{1,1,3}$. Since we solve the linear system (74)–(76) using a Schur complement for $\hat{p}_h$, we will report in this section the size of the Schur complement matrix, i.e., dimM_r, rather than the size of dim$(\mathbf{V}_r \times W_r)$.

In Tables 2–3, we present the errors and the orders of the convergence for the lowest two indices of the full $H(\mathrm{div})$-approximation spaces RT, AT, and ABF; although, we omit ABF$_1$ because the sheer size of its linear system is computationally excessive. On cubical meshes $\mathscr{T}_h^1$, RT$_0$ and AT$_0$ coincide. Table 2 shows first order approximation of the scalar p, the vector $\mathbf{u}$, and the divergence $\nabla \cdot \mathbf{u}$, as we should expect. The ABF$_0$ space gives higher order approximation of all three variables on cubes because it is constructed with higher order polynomials and, in fact, includes RT$_1$. The results for RT$_1$ and AT$_1$ (which are different spaces even on cubical meshes) show second order convergence for all the variables. The errors for RT$_1$ are smaller than AT$_1$, but RT$_1$ uses more degrees of freedom, both locally and globally.

Table 3 shows that for the hexahedral mesh sequence $\mathscr{T}_h^3$, RT$_0$ retains first order convergence of the scalar but loses convergence of the vector and divergence, while AT$_0$ shows first order convergence for all three quantities. The ABF$_0$ space still gives a higher order convergence rate for the scalar on the meshes tested. However, we can observe that the vector and divergence approximations quickly decrease to first order. We also observe that AT$_1$ gives the optimal second order approximation of all quantities, whereas RT$_1$ only retains second order for the scalar. The vector reduces to first order in this numerical test, but the results on the definition of ABF$_0$ [6] show that this first order convergence cannot be ensured on general meshes. The divergence appears to be converging at less than first order.

Table 2 Errors and orders of convergence for low order RT, AT, and ABF spaces on cubical meshes.

		M_r	$\|p - p_h\|$		$\|\mathbf{u} - \mathbf{u}_h\|$		$\|\nabla \cdot (\mathbf{u} - \mathbf{u}_h)\|$	
n	n^3	DOFs	error	order	error	order	error	order
RT$_0$ = AT$_0$ on $\mathscr{T}_h^1$ meshes
2	8	36	2.417e-1		1.136e-0		7.156e-0	
6	216	756	9.110e-2	0.95	4.078e-1	0.97	2.697e-0	0.95
12	1728	5616	4.609e-2	0.99	2.052e-1	0.99	1.365e-0	0.99
24	13824	43200	2.312e-2	1.00	1.027e-1	1.00	6.844e-1	1.00
ABF$_0$ on $\mathscr{T}_h^1$ meshes
2	8	144	1.035e-2		2.523e-1		2.578e-1	
6	216	3024	2.961e-4	3.17	2.786e-2	2.01	8.389e-3	3.06
12	1728	22464	3.523e-5	3.05	6.953e-3	2.00	1.031e-3	3.02
24	13824	172800	4.345e-6	3.01	1.737e-3	2.00	1.283e-4	3.00
RT$_1$ on $\mathscr{T}_h^1$ meshes
2	8	144	5.419e-2		2.440e-1		1.603e-0	
6	216	3024	6.231e-3	1.99	2.773e-2	1.99	1.845e-1	1.99
12	1728	22464	1.562e-3	2.00	6.945e-3	2.00	4.626e-2	2.00
24	13824	172800	3.909e-4	2.00	1.737e-3	2.00	1.157e-2	2.00
AT$_1$ on $\mathscr{T}_h^1$ meshes
2	8	108	1.171e-1		4.358e-1		3.465e-0	
6	216	2268	1.505e-2	1.94	5.164e-2	1.98	4.455e-1	1.94
12	1728	16848	3.814e-3	1.99	1.298e-2	1.99	1.129e-1	1.99
24	13824	129600	9.567e-4	2.00	3.249e-3	2.00	2.833e-2	2.00

6.2 Reduced $H(\mathrm{div})$-approximation spaces

Next we consider the reduced H(div)-approximation spaces BDDF$_1$ and AT$_1^{\mathrm{red}}$, which coincide on cubical meshes. These spaces have the same local and global dimension, as shown in Table 4. The computational results appear in Tables 5–6. As we expect, the elements give first order approximation for the scalar p and the divergence $\nabla \cdot \mathbf{u}$ and second order convergence for the vector $\mathbf{u}$ on cubical meshes, as shown in Table 5. On the hexahedral meshes $\mathscr{T}_h^3$, Table 6 shows that BDDF$_1$ has first order approximation of the scalar but loses convergence of the vector and the divergence. When AT$_1^{\mathrm{red}}$ is used instead, the optimal convergence rates of the cubical meshes are recovered for the hexahedral meshes, i.e., second order approximation for the vector $\mathbf{u}$ and first order for the scalar p and the divergence $\nabla \cdot \mathbf{u}$.

7 Conclusions

We generalized the two dimensional mixed finite elements of Arbogast and Correa [1] defined on quadrilaterals to three dimensional cuboidal hexahedra. Our construction is similar in that vector polynomials are used directly on the element. The space of polynomials used is rich enough to give good approximation properties over the element for both the vector variable and its divergence (as either full or reduced $H(\mathrm{div})$-approximation). Unfortunately, the traces of the normal components of these vector polynomials onto the faces do not independently span the full space of polynomials. This property is needed for $H(\mathrm{div})$-conformity. Therefore, supplemental functions are added to the space to give the full set of edge degrees of freedom (i.e., normal fluxes).

Table 3 Errors and orders of convergence for low order RT, AT, and ABF spaces on $\mathcal{T}_h^3$ meshes.

n	n^3	M_r DOFs	$\|p - p_h\|$ error	order	$\|\mathbf{u} - \mathbf{u}_h\|$ error	order	$\|\nabla \cdot (\mathbf{u} - \mathbf{u}_h)\|$ error	order
			RT$_0$ on $\mathcal{T}_h^3$ meshes					
2	8	36	2.660e-1		1.185e-0		7.488e-0	
6	216	756	9.464e-2	0.94	4.591e-1	0.86	3.149e-0	0.76
12	1728	5616	4.782e-2	0.99	2.630e-1	0.75	1.952e-0	0.60
24	13824	43200	2.400e-2	1.00	1.838e-1	0.45	1.530e-0	0.29
			AT$_0$ on $\mathcal{T}_h^3$ meshes					
2	8	36	2.661e-1		1.226e-0		7.873e-0	
6	216	756	9.452e-2	0.94	4.275e-1	0.96	2.798e-0	0.94
12	1728	5616	4.771e-2	0.99	2.150e-1	0.99	1.413e-0	0.99
24	13824	43200	2.394e-2	1.00	1.077e-1	1.00	7.087e-1	1.00
			ABF$_0$ on $\mathcal{T}_h^3$ meshes					
2	8	144	1.474e-2		2.815e-1		3.649e-1	
6	216	3024	4.706e-4	3.04	3.697e-2	1.85	2.222e-2	2.33
12	1728	22464	6.438e-5	2.85	1.310e-2	1.47	5.909e-3	1.77
24	13824	172800	9.937e-6	2.65	5.537e-3	1.19	2.261e-3	1.30
			RT$_1$ on $\mathcal{T}_h^3$ meshes					
2	8	144	5.644e-2		2.754e-1		1.996e-0	
6	216	3024	7.098e-3	2.03	3.688e-2	1.83	2.834e-1	1.69
12	1728	22464	1.814e-3	2.00	1.311e-2	1.47	1.239e-1	1.15
24	13824	172800	4.541e-4	2.00	5.547e-3	1.19	7.382e-2	0.64
			AT$_1$ on $\mathcal{T}_h^3$ meshes					
2	8	108	1.299e-1		4.526e-1		3.846e-0	
6	216	2268	1.600e-2	1.95	5.629e-2	2.00	4.737e-1	1.95
12	1728	16848	4.091e-3	1.98	1.436e-2	1.99	1.211e-1	1.98
24	13824	129600	1.027e-3	2.00	3.600e-3	2.00	3.040e-2	2.00

Table 4 The dimensions of the local BDDF and AT$^{\text{red}}$ spaces on a hexahedron E. These spaces coincide on rectangles, and they have the same local dimension. Only the AT$^{\text{red}}$ spaces give optimal order convergence on hexahedra.

	BDDF, AT$_r^{\text{red}}$
$\dim\mathbf{V}(E)$	$\frac{1}{2}(r+1)(r+2)(r+3) + 3(r+1)$
$\dim W(E)$	$\frac{1}{6}r(r+1)(r+2)$
$r = 1$	$18 + 1$

Table 5 Errors and orders of convergence for BDDF$_1$ and AT$_1^{\text{red}}$.

n	n^3	M_r DOF	$\|p - p_h\|$ error	order	$\|\mathbf{u} - \mathbf{u}_h\|$ error	order	$\|\nabla \cdot (\mathbf{u} - \mathbf{u}_h)\|$ error	order
			BDDF$_1$ = AT$_1^{\text{red}}$ on $\mathcal{T}_h^1$ meshes					
2	8	108	2.417e-1		5.611e-1		7.156e-0	
6	216	2268	9.114e-2	0.95	8.601e-2	1.85	2.697e-0	0.95
12	1728	16848	4.610e-2	0.99	2.249e-2	1.95	1.365e-0	0.99
24	13824	129600	2.312e-2	1.00	5.701e-3	1.98	6.844e-1	1.00

Table 6 Errors and orders of convergence for BDDF$_1$ and AT$_1^{\text{red}}$.

n	n^3	M_r DOF	$\|p - p_h\|$ error	order	$\|\mathbf{u} - \mathbf{u}_h\|$ error	order	$\|\nabla \cdot (\mathbf{u} - \mathbf{u}_h)\|$ error	order
			BDDF$_1$ on $\mathscr{T}_h^3$ meshes					
2	8	108	2.665e-1		6.450e-1		7.487e-0	
6	216	2268	9.481e-2	0.94	1.164e-1	1.52	3.149e-0	0.76
12	1728	16848	4.786e-2	0.99	4.000e-2	1.43	1.952e-0	0.60
24	13824	129600	2.401e-2	1.00	1.723e-2	1.16	1.530e-0	0.29
			AT$_1^{\text{red}}$ on $\mathscr{T}_h^3$ meshes					
2	8	108	2.660e-1		6.435e-1		7.876e-0	
6	216	2268	9.455e-2	0.94	9.760e-2	1.76	2.798e-0	0.94
12	1728	16848	4.772e-2	0.99	2.610e-2	1.91	1.413e-0	0.99
24	13824	129600	2.394e-2	1.00	6.753e-3	1.96	7.087e-1	1.00

These supplemental functions are defined on a reference element and mapped to the hexahedron using the Piola transform.

We provided a systematic procedure for defining supplemental functions that are divergence-free and have any prescribed polynomial normal flux in Sections 3–4. This is the key contribution of this work.

We also discussed in Section 5 what normal fluxes are required of the supplemental functions to define mixed finite element spaces. These supplemental functions are then defined using functions from Section 4. When index $r = 0$ (the lowest order case), we gave two possibilities. The simple case has shape functions defined by the explicit formulas (37)–(42). The more general case for $r = 0$ in Section 5.1.2 requires a bit of local linear algebra, (43)–(46), to determine the fluxes required of the supplemental functions (47)–(48). For $r = 1$, we gave three possibilities: (1) for elements that satisfy the invertibility condition (63), such as elements with two parallel faces or that are truncated pillars; (2) for elements with a prescribed normal flux (up to two parameters, which must be set appropriately); and (3) for the general case of Section 5.3, which applies to all $r \geq 1$. The general case requires some local linear algebra to determine the fluxes required of the supplemental functions.

Numerical results in Section 6 verified that our approach produces mixed finite elements that achieve optimal full or reduced $H(\text{div})$-approximation on quadrilateral meshes.

A On the invertibility of matrix $\mathbf{C} \circ \mathbf{H}$

In Section 5.2 Theorem 2, we stated that the independence of the degrees of freedom of our new spaces when $r = 1$ with symmetric supplements reduces to the invertibility of the matrix $\mathbf{C} \circ \mathbf{H}$ (63), which is the Hadamard product of the centroid matrix $\mathbf{C}$ (see (80)) and the normal matrix $\mathbf{H}$ (see (77)) for faces f_1, f_3, and f_5. In this section, we discuss the properties of these matrices and how they relate to the geometry of the convex hexahedron $\tilde{E}$. We then prove the invertibility of $\mathbf{C} \circ \mathbf{H}$ in two special cases.
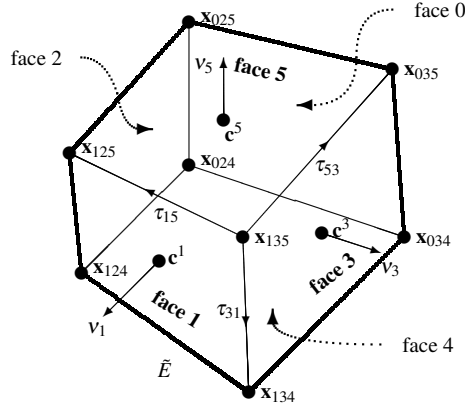
Fig. 3 The geometry of $\tilde{E}$.

A.1 The face normal matrix **H**

Following the discussion in Section 5.2, we know that any convex cuboidal hexahedron can be affinely mapped to a simpler shape $\tilde{E}$, for which $v_0 = -\mathbf{e}_1$, $v_2 = -\mathbf{e}_2$, $v_4 = -\mathbf{e}_3$ and $\mathbf{x}_{124} = \mathbf{e}_1$, $\mathbf{x}_{034} = \mathbf{e}_2$, $\mathbf{x}_{025} = \mathbf{e}_3$. Therefore, the normal fluxes v_1, v_3, v_5 fully define the geometry of $\tilde{E}$. We define the face normal matrix

$$\mathbf{H} = \begin{bmatrix} v_{1,1} & v_{3,1} & v_{5,1} \\ v_{1,2} & v_{3,2} & v_{5,2} \\ v_{1,3} & v_{3,3} & v_{5,3} \end{bmatrix}. \tag{77}$$

The cross product of the normals of two intersecting faces is parallel to the edge of intersection. Let $\tau_{ij} = v_i \times v_j$, where $\|v_i \times v_j\| > 0$ for two intersecting faces. For example (see Figure 3), $\tau_{31} = -\tau_{13}$ points from $\mathbf{x}_{135}$ to $\mathbf{x}_{134}$.

Theorem 4 *For any convex hexahedron $\tilde{E}$, all principle minors of **H** are strictly positive.*

Proof We use the fact that for three vectors,

$$(\mathbf{a} \times \mathbf{b}) \times (\mathbf{a} \times \mathbf{c}) = ((\mathbf{b} \times \mathbf{c}) \cdot \mathbf{a})\,\mathbf{a} = \det[\mathbf{a}\ \mathbf{b}\ \mathbf{c}]\,\mathbf{a}.$$

We first show that $\det(\mathbf{H}) > 0$. Consider face 5 in Figure 3, for which

$$\tau_{53} \times \tau_{15} = (v_5 \times v_3) \times (v_1 \times v_5) = (v_5 \times v_1) \times (v_5 \times v_3) = \det(\mathbf{H})v_5. \tag{78}$$

It is obvious that $(\tau_{53} \times \tau_{15}) \cdot v_5 > 0$ when face 5 is a convex quadrilateral, i.e., the triangle with vertices $\mathbf{x}_{135}$, $\mathbf{x}_{125}$ and $\mathbf{x}_{035}$ does not degenerate; therefore, $\det(\mathbf{H}) > 0$.

Second, we show that the diagonal entries of **H** are strictly positive. By convexity, on face 5, $(\tau_{52} \times \tau_{05}) \cdot v_5 > 0$. Thus, computing as in (78), we see that $(v_0 \times v_2) \cdot v_5 > 0$. Since $v_0 \times v_2 = (-\mathbf{e}_1) \times (-\mathbf{e}_2) = \mathbf{e}_3$, we obtain that $v_{5,3} > 0$. Similarly, since $(\tau_{14} \times \tau_{21}) \cdot v_1 > 0$ and $(\tau_{30} \times \tau_{43}) \cdot v_2 > 0$, we have $v_{1,1} > 0$ and $v_{3,2} > 0$.

Finally, we show that the principal minors of order 2 are strictly positive. By convexity, we have on face 5, $(\tau_{50} \times \tau_{35}) \cdot v_5 > 0$, and so $(v_3 \times v_0) \cdot v_5 > 0$, i.e.,

$$\det \begin{bmatrix} v_{3,1} & -1 & v_{5,1} \\ v_{3,2} & 0 & v_{5,2} \\ v_{3,3} & 0 & v_{5,3} \end{bmatrix} = \det \begin{bmatrix} v_{3,2} & v_{5,2} \\ v_{3,3} & v_{5,3} \end{bmatrix} > 0. \tag{79}$$

The other two principal minors of order 2 can be shown from $(\tau_{51} \times \tau_{25}) \cdot v_5 > 0$ and $(\tau_{13} \times \tau_{41}) \cdot v_1 > 0$.

A.2 The face centroids and matrix $\mathbf{C}$

In this section, we look at the matrix

$$\mathbf{C} = \begin{bmatrix} c_1^1 & c_1^3 & c_1^5 \\ c_2^1 & c_2^3 & c_2^5 \\ c_3^1 & c_3^3 & c_3^5 \end{bmatrix} = [\mathbf{c}^1 \, \mathbf{c}^3 \, \mathbf{c}^5], \tag{80}$$

where c_ℓ^i is the average over face i of the variable x_ℓ. That is, $\mathbf{c}^1$, $\mathbf{c}^3$, $\mathbf{c}^5$ are the face centroids of faces 1, 3, and 5, respectively. Obviously, all c_ℓ^i are strictly positive.

Let $\mathbf{Proj}^3 : \mathbb{R}^3 \to \mathbb{R}^2$ denote the projection in the direction $\mathbf{e}_3$ to the $(x_1, x_2)-$plane. Therefore, $\mathbf{Proj}^3(\mathbf{c}^i)$ is the centroid of the projected face i, $\mathbf{Proj}^3(f_i)$, $i = 1, 3, 5$.

Lemma 3 *If face $2i$ and face $2i+1$, $i = 0, 1, 2$, are parallel, then the determinant of the principal minor of $\mathbf{C}$ formed by deleting row and column $i+1$ is strictly positive.*

Proof Without loss of generality, we only need to show that when $v_5 = \mathbf{e}_3$,

$$\det \begin{bmatrix} c_1^1 & c_1^3 \\ c_2^1 & c_2^3 \end{bmatrix} > 0. \tag{81}$$

When $v_5 = \mathbf{e}_3$, τ_{53} and τ_{34} are parallel, as are τ_{15} and τ_{41}. See Figure 4 for the projected view of $\tilde{E}$. From the figure, the area of the triangle formed by $\mathbf{x}_{024}$, $\mathbf{Proj}^3(\mathbf{c}^1)$ and $\mathbf{Proj}^3(\mathbf{c}^3)$ is positive, so

$$\left(\begin{pmatrix} c_1^1 \\ c_2^1 \\ 0 \end{pmatrix} \times \begin{pmatrix} c_1^3 \\ c_2^3 \\ 0 \end{pmatrix} \right) \cdot \mathbf{e}_3 > 0, \tag{82}$$
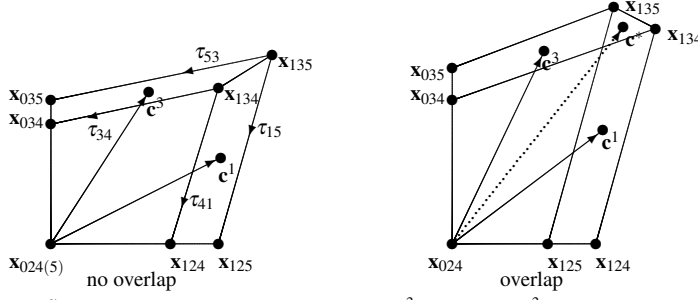
which is (81).

Fig. 4 View of $\tilde{E}$ from the top. The two cases are for $\mathbf{Proj}^3(f_1)$ and $\mathbf{Proj}^3(f_3)$ overlap or not.

A.3 Invertibility of $\mathbf{C} \circ \mathbf{H}$

We have affinely mapped our convex, cuboidal hexahedron E to $\tilde{E}$. An affine transformation will take parallel lines to parallel lines. Therefore, if E has two pair of parallel faces, or if E is a truncated pillar, the same will be true of $\tilde{E}$.

Theorem 5 *For a convex, cuboidal hexahedron $\tilde{E}$, if one pair of opposite faces are parallel, then the matrix $\mathbf{C} \circ \mathbf{H}$ is invertible.*

Proof Without loss of generality, we assume that face 4 is parallel to face 5. Therefore $v_{5,1} = v_{5,2} = 0$ and by Theorem 4 we know that $v_{5,3} > 0$. The invertibility of matrix $\mathbf{C} \circ \mathbf{H}$ is reduced to showing that

$$\det \begin{bmatrix} c_1^1 v_{1,1} & c_1^3 v_{3,1} \\ c_2^1 v_{1,2} & c_2^3 v_{3,2} \end{bmatrix} > 0. \tag{83}$$

By Lemma 3, we know that $c_1^1 c_2^3 > c_2^1 c_1^3 > 0$. By Theorem 4, we have $v_{1,1} v_{3,2} > v_{1,2} v_{3,1}$. Therefore, $c_1^1 c_2^3 v_{1,1} v_{3,2} > c_2^1 c_1^3 v_{1,2} v_{3,1}$, and (83) holds.

Theorem 6 *For any truncated pillar $\tilde{E}$, the matrix $\mathbf{C} \circ \mathbf{H}$ is invertible.*

Proof We assume without loss of generality that $\tilde{E}$ is a truncated vertical pillar, so $v_{0,3} = v_{1,3} = v_{2,3} = v_{3,3} = 0$. The matrix $\mathbf{C} \circ \mathbf{H}$ reduces to

$$\mathbf{C} \circ \mathbf{H} = \begin{bmatrix} c_1^1 v_{1,1} & c_1^3 v_{3,1} & c_1^5 v_{5,1} \\ c_2^1 v_{1,2} & c_2^3 v_{3,2} & c_2^5 v_{5,2} \\ 0 & 0 & c_3^5 v_{5,3} \end{bmatrix}. \tag{84}$$

Moreover, the projection of $\mathbf{c}^1$ on the bottom plane is in the line from $\mathbf{x}_{124}$ to $\mathbf{x}_{134}$, and the projection of $\mathbf{c}^3$ in the line from $\mathbf{x}_{134}$ to $\mathbf{x}_{034}$ (see Figure 4, where now $\mathbf{x}_{035}$ and $\mathbf{x}_{034}$ are on top of each other, as are $\mathbf{x}_{134}$ and $\mathbf{x}_{135}$, and also $\mathbf{x}_{124}$ and $\mathbf{x}_{125}$). Therefore, we have

$$\det \begin{bmatrix} c_1^1 & c_1^3 \\ c_2^1 & c_2^3 \end{bmatrix} > 0. \tag{85}$$

The rest of the proof follows that of Theorem 5.

B Proof of Theorem 2

For $\tilde{E}$, the local variables on face 1 are x_2 and x_3, so a base for the normal flux on f_1 is $\text{span}\{1, x_2, x_3\} = \mathbb{P}_1(f_1)$. Similarly, $\text{span}\{1, x_1, x_3\} = \mathbb{P}_1(f_3)$, and $\text{span}\{1, x_1, x_2\} = \mathbb{P}_1(f_5)$. Define the operator $\mathscr{F}_{135}^* \in \mathbb{R}^{1 \times 9}$ to be the normal fluxes of f_1, f_3, and f_5 in the local degrees of freedom, i.e.,

$$\mathscr{F}_{135}^*(\mathbf{u})\mathbf{X}^T = \mathscr{F}_{135}(\mathbf{u}), \quad \text{where} \quad \mathbf{X} = \begin{bmatrix} 1 \ x_2 \ x_3 \big| 1 \ x_1 \ x_3 \big| 1 \ x_1 \ x_2 \end{bmatrix}. \tag{86}$$

Similarly, we define $\mathscr{F}_{135}^*(\mathbf{u}_1, \dots, \mathbf{u}_n) = \begin{pmatrix} \mathscr{F}_{135}^*(\mathbf{u}_1) \\ \vdots \\ \mathscr{F}_{135}^*(\mathbf{u}_n) \end{pmatrix} \in \mathbb{R}^{n \times 9}$. On f_1, $(\mathbf{x} - \mathbf{e}_1) \cdot v_1 = 0$, i.e., $x_1 v_{1,1} = v_{1,1} - x_2 v_{1,2} - x_3 v_{1,3}$. Similar statements hold on f_3 and f_5, so we can rewrite (60) as

$$\mathscr{F}_{135}^*(\psi_9^*, \psi_{10}^*, \psi_{11}^*) = \begin{bmatrix} v_{1,1} & -v_{1,2} & -v_{1,3} & 0 & v_{3,1} & 0 & 0 & v_{5,1} & 0 \\ 0 & v_{1,2} & 0 & v_{3,2} & -v_{3,1} & -v_{3,3} & 0 & 0 & v_{5,2} \\ 0 & 0 & v_{1,3} & 0 & 0 & v_{3,3} & v_{5,3} & -v_{5,1} & -v_{5,2} \end{bmatrix}. \tag{87}$$

To prove that (62) provides independent degrees of freedom, we need to show that the 9×9 matrix

$$\mathscr{F}_{135}^*(\psi_9^*, \dots, \psi_{11}^*, \sigma_0, \dots, \sigma_5)$$

$$= \begin{bmatrix} v_{1,1} & -v_{1,2} & -v_{1,3} & 0 & v_{3,1} & 0 & 0 & v_{5,1} & 0 \\ 0 & v_{1,2} & 0 & v_{3,2} & -v_{3,1} & -v_{3,3} & 0 & 0 & v_{5,2} \\ 0 & 0 & v_{1,3} & 0 & 0 & v_{3,3} & v_{5,3} & -v_{5,1} & -v_{5,2} \\ -c_2^1 & 1 & 0 & 0 & 0 & 0 & 0 & 0 & 0 \\ -c_3^1 & 0 & 1 & 0 & 0 & 0 & 0 & 0 & 0 \\ 0 & 0 & 0 & -c_1^3 & 1 & 0 & 0 & 0 & 0 \\ 0 & 0 & 0 & -c_3^3 & 0 & 1 & 0 & 0 & 0 \\ 0 & 0 & 0 & 0 & 0 & 0 & -c_1^5 & 1 & 0 \\ 0 & 0 & 0 & 0 & 0 & 0 & -c_2^5 & 0 & 1 \end{bmatrix} \tag{88}$$

is invertible. By the fact that $\mathbf{c}^i = [c_1^i \ c_2^i \ c_3^i]^T$ is on f_i, $i = 1, 3, 5$, we know that, e.g., $c_1^1 v_{1,1} = v_{1,1} - c_2^1 v_{1,2} - c_3^1 v_{1,3}$. In (88), using rows 4 to 9 to cancel out entries in columns 2, 3, 5, 6, 8, and 9 of the first three rows, we obtain

$$\begin{bmatrix} c_1^1 v_{1,1} & 0 & 0 & c_1^3 v_{3,1} & 0 & 0 & c_1^5 v_{5,1} & 0 & 0 \\ c_2^1 v_{1,2} & 0 & 0 & c_2^3 v_{3,2} & 0 & 0 & c_2^5 v_{5,2} & 0 & 0 \\ c_3^1 v_{1,3} & 0 & 0 & c_3^3 v_{3,3} & 0 & 0 & c_3^5 v_{5,3} & 0 & 0 \\ -c_2^1 & 1 & 0 & 0 & 0 & 0 & 0 & 0 & 0 \\ -c_3^1 & 0 & 1 & 0 & 0 & 0 & 0 & 0 & 0 \\ 0 & 0 & 0 & -c_1^3 & 1 & 0 & 0 & 0 & 0 \\ 0 & 0 & 0 & -c_3^3 & 0 & 1 & 0 & 0 & 0 \\ 0 & 0 & 0 & 0 & 0 & 0 & -c_1^5 & 1 & 0 \\ 0 & 0 & 0 & 0 & 0 & 0 & -c_2^5 & 0 & 1 \end{bmatrix}.$$

We rearrange the columns to

$$
\left[
\begin{array}{ccc|cccccc}
c_1^1 v_{1,1} & c_1^3 v_{3,1} & c_1^5 v_{5,1} & 0 & 0 & 0 & 0 & 0 & 0 \\
c_2^1 v_{1,2} & c_2^3 v_{3,2} & c_2^5 v_{5,2} & 0 & 0 & 0 & 0 & 0 & 0 \\
c_3^1 v_{1,3} & c_3^3 v_{3,3} & c_3^5 v_{5,3} & 0 & 0 & 0 & 0 & 0 & 0 \\
\hline
-c_2^1 & 0 & 0 & 1 & 0 & 0 & 0 & 0 & 0 \\
-c_3^1 & 0 & 0 & 0 & 1 & 0 & 0 & 0 & 0 \\
0 & -c_1^3 & 0 & 0 & 0 & 1 & 0 & 0 & 0 \\
0 & -c_3^3 & 0 & 0 & 0 & 0 & 1 & 0 & 0 \\
0 & 0 & -c_1^5 & 0 & 0 & 0 & 0 & 1 & 0 \\
0 & 0 & -c_2^5 & 0 & 0 & 0 & 0 & 0 & 1 \\
\end{array}
\right].
$$

The upper left submatrix is exactly $\mathbf{C} \circ \mathbf{H}$, and the proof of Theorem 2 is complete.

C Proof of Theorem 1

Rewrite (61) with $\mathscr{F}_{135}^*$, to obtain

$$
\mathscr{F}_{135}^*(\psi_9^*,\dots,\psi_{11}^*,\sigma_0,\dots,\sigma_3,\sigma_4^*,\sigma_5^*)
$$

$$
=
\left[
\begin{array}{ccc|ccc|ccc}
v_{1,1} & -v_{1,2} & -v_{1,3} & 0 & v_{3,1} & 0 & 0 & v_{5,1} & 0 \\
0 & v_{1,2} & 0 & v_{3,2} & -v_{3,1} & -v_{3,3} & 0 & 0 & v_{5,2} \\
0 & 0 & v_{1,3} & 0 & 0 & v_{3,3} & v_{5,3} & -v_{5,1} & -v_{5,2} \\
\hline
-c_2^1 & 1 & 0 & 0 & 0 & 0 & 0 & 0 & 0 \\
-c_3^1 & 0 & 1 & 0 & 0 & 0 & 0 & 0 & 0 \\
\hline
0 & 0 & 0 & -c_1^3 & 1 & 0 & 0 & 0 & 0 \\
0 & 0 & 0 & -c_3^3 & 0 & 1 & 0 & 0 & 0 \\
\hline
\dfrac{-|f_5|c_1^5+t}{|f_1|} & 0 & 0 & \dfrac{-t}{|f_3|} & 0 & 0 & 0 & 1 & 0 \\
\dfrac{-s}{|f_1|} & 0 & 0 & \dfrac{-|f_5|c_2^5+s}{|f_3|} & 0 & 0 & 0 & 0 & 1 \\
\end{array}
\right]. \quad (89)
$$

If there exist constants s and t such that the matrix (89) is invertible, the non-symmetric supplements σ_0 to σ_3, σ_4^*, and σ_5^* provide independent degrees of freedom.

Using rows 4 to 7 to cancel out entries in columns 2, 3, 5, and 6 in the first three rows, we obtain

$$
\left[
\begin{array}{ccc|ccc|ccc}
c_1^1 v_{1,1} & 0 & 0 & c_1^3 v_{3,1} & 0 & 0 & 0 & v_{5,1} & 0 \\
c_2^1 v_{1,2} & 0 & 0 & c_2^3 v_{3,2} & 0 & 0 & 0 & 0 & v_{5,2} \\
c_3^1 v_{1,3} & 0 & 0 & c_3^3 v_{3,3} & 0 & 0 & v_{5,3} & -v_{5,1} & -v_{5,2} \\
\hline
-c_2^1 & 1 & 0 & 0 & 0 & 0 & 0 & 0 & 0 \\
-c_3^1 & 0 & 1 & 0 & 0 & 0 & 0 & 0 & 0 \\
\hline
0 & 0 & 0 & -c_1^3 & 1 & 0 & 0 & 0 & 0 \\
0 & 0 & 0 & -c_3^3 & 0 & 1 & 0 & 0 & 0 \\
\hline
(-|f_5|c_1^5+t)/|f_1| & 0 & 0 & -t/|f_3| & 0 & 0 & 0 & 1 & 0 \\
-s/|f_1| & 0 & 0 & (-|f_5|c_2^5+s)/|f_3| & 0 & 0 & 0 & 0 & 1 \\
\end{array}
\right].
$$

Rearrange the columns and rows to see

$$
\left[
\begin{array}{cccc|ccccc}
c_1^1 v_{1,1} & c_1^3 v_{3,1} & v_{5,1} & 0 & 0 & 0 & 0 & 0 & 0 \\
c_2^1 v_{1,2} & c_2^3 v_{3,2} & 0 & v_{5,2} & 0 & 0 & 0 & 0 & 0 \\
(-|f_5|c_1^5+t)/|f_1| & -t/|f_3| & 1 & 0 & 0 & 0 & 0 & 0 & 0 \\
-s/|f_1| & (-|f_5|c_2^5+s)/|f_3| & 0 & 1 & 0 & 0 & 0 & 0 & 0 \\
\hline
c_3^1 v_{1,3} & c_3^3 v_{3,3} & -v_{5,1} & -v_{5,2} & v_{5,3} & 0 & 0 & 0 & 0 \\
-c_2^1 & 0 & 0 & 0 & 0 & 1 & 0 & 0 & 0 \\
-c_3^1 & 0 & 0 & 0 & 0 & 0 & 1 & 0 & 0 \\
0 & -c_1^3 & 0 & 0 & 0 & 0 & 0 & 1 & 0 \\
0 & -c_3^3 & 0 & 0 & 0 & 0 & 0 & 0 & 1
\end{array}
\right].
$$

This matrix is invertible if and only if

$$
\left[
\begin{array}{cc|cc}
c_1^1 v_{1,1} & c_1^3 v_{3,1} & v_{5,1} & 0 \\
c_2^1 v_{1,2} & c_2^3 v_{3,2} & 0 & v_{5,2} \\
\hline
(-|f_5|c_1^5+t)/|f_1| & -t/|f_3| & 1 & 0 \\
-s/|f_1| & (-|f_5|c_2^5+s)/|f_3| & 0 & 1
\end{array}
\right]
\tag{90}
$$

is invertible. A 2×2 block matrix has the following lemma [18].

Lemma 4 *If* $\mathbf{M} = \begin{pmatrix} \mathbf{A} & \mathbf{B} \\ \mathbf{C} & \mathbf{D} \end{pmatrix}$, *where* $\mathbf{A}$, $\mathbf{B}$, $\mathbf{C}$, $\mathbf{D} \in \mathbb{R}^{n \times n}$ *and* $\mathbf{CD} = \mathbf{DC}$, *then*

$$
\det \mathbf{M} = \det(\mathbf{AD} - \mathbf{BC}).
$$

Obviously, the lower right submatrix of (90) (an identity matrix) commutes with any 2×2 matrix. Thus, to prove that matrix (90) is invertible, we need to show that

$$
\det \begin{bmatrix} c_1^1 v_{1,1} + v_{5,1}(|f_5|c_1^5 - t)/|f_1| & c_1^3 v_{3,1} + t\, v_{5,1}/|f_3| \\ c_2^1 v_{1,2} + s\, v_{5,2}/|f_1| & c_2^3 v_{3,2} + v_{5,2}(|f_5|c_2^5 - s)/|f_3| \end{bmatrix} \neq 0.
\tag{91}
$$

This determinant is a bilinear function in s and t, denoted as $d(s,t)$. If we can prove that $d(s,t) \not\equiv 0$, then we can find a pair (s^*, t^*) such that $d(s^*, t^*) \neq 0$, and the last two non-symmetric supplements σ_4^* and σ_5^* in (61) are defined. There are two cases.

    Case 1: $v_{5,1} = 0$ and $v_{5,2} = 0$. In this case, $\tilde{E}$ is a truncated vertical pillar, and by the proof of Theorem 6, we know that

$$
d(s,t) = \det \begin{bmatrix} c_1^1 v_{1,1} & c_1^3 v_{3,1} \\ c_2^1 v_{1,2} & c_2^3 v_{3,2} \end{bmatrix} > 0,
\tag{92}
$$

and s and t may be taken arbitrarily.

    Case 2: $v_{5,2} \neq 0$ or $v_{5,1} \neq 0$. By symmetry, we only show the situation $v_{5,2} \neq 0$ here. Let

$$
a = d(0,0) = \det \begin{bmatrix} c_1^1 v_{1,1} + v_{5,1}(|f_5|c_1^5)/|f_1| & c_1^3 v_{3,1} \\ c_2^1 v_{1,2} & c_2^3 v_{3,2} + v_{5,2}(|f_5|c_2^5)/|f_3| \end{bmatrix},
\tag{93}
$$

$$
b = d(|f_5|c_2^5, 0) = \det \begin{bmatrix} c_1^1 v_{1,1} + v_{5,1}(|f_5|c_1^5)/|f_1| & c_1^3 v_{3,1} \\ c_2^1 v_{1,2} + v_{5,2}(|f_5|c_2^5)/|f_1| & c_2^3 v_{3,2} \end{bmatrix}.
\tag{94}
$$

Then

$$a - b = (v_{5,2}|f_5|c_2^5) \det \begin{bmatrix} c_1^1 v_{1,1} + v_{5,1}(|f_5|c_1^5)/|f_1| & c_1^3 v_{3,1} \\ -1/|f_1| & 1/|f_3| \end{bmatrix}$$

$$= \frac{v_{5,2}|f_5|c_2^5}{|f_1||f_3|} (|f_1|c_1^1 v_{1,1} + |f_3|c_1^3 v_{3,1} + |f_5|c_1^5 v_{5,1}) \neq 0, \tag{95}$$

since

$$|f_1|c_1^1 v_{1,1} + |f_3|c_1^3 v_{3,1} + |f_5|c_1^5 v_{5,1} \tag{96}$$

$$= \int_{\partial \tilde{E}} \begin{pmatrix} x_1 \\ 0 \\ 0 \end{pmatrix} \cdot v \, dA = \int_{\tilde{E}} \nabla \cdot \begin{pmatrix} x_1 \\ 0 \\ 0 \end{pmatrix} dV = |\tilde{E}| \neq 0.$$

The fact $a \neq b$ implies that $d(s,t) \not\equiv 0$, and so (89) is invertible.

References

1. Arbogast, T., Correa, M.R.: Two families of H(div) mixed finite elements on quadrilaterals of minimal dimension. SIAM J. Numer. Anal. **54**(6), 3332–3356 (2016). DOI 10.1137/15M1013705
2. Arnold, D.N., Awanou, G.: Finite element differential forms on cubical meshes. Math. Comp. **83**, 1551–1570 (2014)
3. Arnold, D.N., Boffi, D., Bonizzoni, F.: Finite element differential forms on curvilinear cubic meshes and their approximation properties. Numer. Math. **129**(1), 1–20 (2015)
4. Arnold, D.N., Boffi, D., Falk, R.S.: Quadrilateral H(div) finite elements. SIAM. J. Numer. Anal. **42**(6), 2429–2451 (2005)
5. Arnold, D.N., Brezzi, F.: Mixed and nonconforming finite element methods: Implementation, post-processing and error estimates. RAIRO Modél. Math. Anal. Numér. **19**, 7–32 (1985)
6. Bergot, M., Duruflé, M.: Approximation of H(div) with high-order optimal finite elements for pyramids, prisms and hexahedra. Communications in Computational Physics **14**(5), 1372–1414 (2013)
7. Brezzi, F., Douglas Jr., J., Duràn, R., Fortin, M.: Mixed finite elements for second order elliptic problems in three variables. Numer. Math. **51**, 237–250 (1987)
8. Brezzi, F., Douglas Jr., J., Marini, L.D.: Two families of mixed elements for second order elliptic problems. Numer. Math. **47**, 217–235 (1985)
9. Brezzi, F., Fortin, M.: Mixed and hybrid finite element methods. Springer-Verlag, New York (1991)
10. Cockburn, B., Fu, G.: Superconvergence by M-decompositions. Part III: Construction of three-dimensional finite elements. ESAIM: Mathematical Modelling and Numerical Analysis **51**(1), 365–398 (2017)
11. Huo-Yuan Duan, H.-Y., Liang, G.-P.: Nonconforming elements in least-squares mixed finite element methods Math. Comp. **73**(245), 1–18 (2004)
12. Falk, R.S., Gatto, P., Monk, P.: Hexahedral H(div) and H(curl) finite elements. ESAIM Math. Model. Numer. Anal. **45**(1), 115–143 (2011)
13. Girault V., Raviart, P.A.: Finite Element Methods for Navier-Stokes Equations: Theory and Algorithms. Springer-Verlag, Berlin (1986)
14. Kwak, D.Y., Pyo H.C.: Mixed finite element methods for general quadrilateral grids. Applied Mathematics and Computation **217**, 6556–6565 (2011)
15. Ponting, D.K.: Corner Point Geometry in Reservoir Simulation. In: P.R. King (eds.) Proc. of the 1st European Conf. on the Mathematics of Oil Recovery, pp. 45–65, Cambridge (1989)
16. Raviart, R.A., Thomas, J.M.: A mixed finite element method for 2nd order elliptic problems. In: I. Galligani, E. Magenes (eds.) Mathematical Aspects of Finite Element Methods, no. 606 in Lecture Notes in Math., pp. 292–315. Springer-Verlag, New York (1977)
17. Shen, J.: Mixed finite element methods on distorted rectangular grids. Tech. Rep. ISC-94-13-MATH, Institute for Scientific Computation, Texas A&M University, College Station, Texas (1994)
18. Silvester, J.R.: Determinants of block matrices. The Mathematical Gazette, 84 (2000)
19. Thomas, J.M.: Sur l'analyse numerique des methodes d'elements finis hybrides et mixtes. Ph.D. thesis, Sciences Mathematiques, à l'Universite Pierre et Marie Curie (1977)